UNIVERSITY OF CALIFORNIA

Santa Barbara

The Contact-Dependent Growth Inhibition Pathways of *Burkholderia pseudomallei* 1026b and *Escherichia coli* EC93

A Thesis submitted in partial satisfaction of the

requirements for the degree Master of Arts

in Molecular, Cellular, and Developmental Biology

by

Natasha Ilyana Edman

Committee in charge:

Professor David A. Low, Chair

Professor Christopher S. Hayes

Professor Stephen J. Poole

September 2015

The thesis of Natasha Ilyana Edman is approved.

_____

Christopher S. Hayes

_____

Stephen J. Poole

_____

David A. Low, Committee Chair

September 2015

The Contact-Dependent Growth Inhibition Pathways of

Burkholderia pseudomallei 1026b and *Escherichia coli* EC93

by

Natasha Ilyana Edman

ACKNOWLEDGMENTS

None of this work would have been possible if it weren't for that fateful day when David Low offered me a position in his lab – scarcely imagining that I would stay for more than four years! David, along with my committee members Christopher Hayes and Stephen Poole, gave me an opportunity that few undergrads receive, and I cannot thank them enough for their feedback, encouragement, and support.

During my time here, I had a series of excellent lab mentors. Fernando Garza-Sánchez, Allison Jones, and Sanna Koskiniemi all took time out of their busy schedules to provide patient and ongoing training; Bruce Braaten gave invaluable technical advice and kept me entertained with his fascinating stories; and Zachary Ruhe generously assisted in design and troubleshooting of several experiments.

I would especially like to acknowledge my three undergrad trainees, Krysten Boggs, Laura Hernandez Santiago, and Matt Stafford, for their enthusiasm, energy, and stoicism in the face of endless serial dilutions. I have had many colleagues who made the Low Lab a special place, among them Stephanie Aoki, Saba Amber, Swarnava Chaudhuri, Licia Dean, Claire t'Kint de Roodenbeke, Sabrina Deuring, Bianca Dunn, Hannah Mills, Anne Otten, Paula Otto-Langereis, Travis Smith, Jaime So, William Tobolowsky, Julia Shimizu Webb, August Williams, and Jing Xiong. The members of the Hayes Lab have been consistently helpful during group meetings and have thrown many excellent barbeques.

Thank you to my grad school classmates, in particular Greg Ekberg, for the now infamous anglerfish presentation. Finally, thanks to Jeffrey Edman, Ursula Edman, and Kevin Kipp for their advice and support, and to Lukas Edman, Maya Edman, and Leo Edman for always bringing a smile to my face (of any shape or size).

ABSTRACT

The Contact-Dependent Growth Inhibition Pathways of

Burkholderia pseudomallei 1026b and *Escherichia coli* EC93

by

Natasha Ilyana Edman

Bacteria engage in social behavior by communicating through a variety of mechanisms. One method of communication is contact-dependent growth inhibition (CDI), a phenomenon in which one bacterium binds and delivers a toxin to a closely related target cell, using the proteins CdiB and CdiA. This toxin blocks cell growth unless the target cell contains an immunity protein, CdiI. The CDI pathway is the process by which toxins are delivered and activated, using distinct target-cell proteins such as outer membrane receptors and inner membrane transporters. The first chapter of this thesis focuses on the CDI system from *Burkholderia pseudomallei* 1026b. We identify three genes whose products appear to be necessary for growth inhibition, and describe a potential CDI pathway for this system. The second chapter discusses the mechanism by which *Escherichia coli* EC93 binds target cells. Mutations in BamA, the $CdiA^{EC93}$ receptor, are described. These mutations confer resistance to CDI and block cell-cell binding. Both chapters demonstrate the variety and species specificity of CDI growth inhibition pathways.

TABLE OF CONTENTS

LIST OF FIGURES

Chapter 1

Genetic analysis of the CDI pathway from Burkholderia pseudomallei 1026b

This is a legal reprint of:

Koskiniemi S, Garza-Sánchez F, Edman N, Chaudhuri S, Poole SJ, Manoil C, Hayes CS,

Low D. Genetic analysis of the CDI pathway from *Burkholderia pseudomallei* 1026b.

PLoS ONE 2015; 10:e0120265.

Abstract

Contact-dependent growth inhibition (CDI) is a mode of inter-bacterial competition mediated by the CdiB/CdiA family of two-partner secretion systems. CdiA binds to receptors on susceptible target bacteria, then delivers a toxin domain derived from its C-terminus. Studies with *Escherichia coli* suggest the existence of multiple CDI growth-inhibition pathways, whereby different systems exploit distinct target-cell proteins to deliver and activate toxins. Here, we explore the CDI pathway in *Burkholderia* using the $CDI_{II}^{Bp1026b}$ system encoded on chromosome II of *Burkholderia pseudomallei* 1026b as a model. We took a genetic approach and selected *Burkholderia thailandensis* E264 mutants that are resistant to growth inhibition by $CDI_{II}^{Bp1026b}$. We identified mutations in three genes, BTH_I0359, BTH_II0599, and BTH_I0986, each of which confers resistance to $CDI_{II}^{Bp1026b}$. BTH_I0359 encodes a small peptide of unknown function, whereas BTH_II0599 encodes a predicted inner membrane transport protein of the major facilitator superfamily. The inner membrane localization of BTH_II0599 suggests that it may facilitate translocation of CdiA-$CT_{II}^{Bp1026b}$ toxin from the periplasm into the cytoplasm of target cells. BTH_I0986 encodes a putative transglycosylase involved in lipopolysaccharide (LPS) synthesis. ΔBTH_I0986 mutants have altered LPS structure and do not interact with CDI^{+} inhibitor cells to the same extent as BTH_I0986^{+} cells, suggesting that LPS could function as a receptor for $CdiA_{II}^{Bp1026b}$. Although ΔBTH_I0359, ΔBTH_II0599, and ΔBTH_I0986 mutations confer resistance to $CDI_{II}^{Bp1026b}$, they provide no protection against the CDI^{E264} system deployed by *B. thailandensis* E264. Together, these findings demonstrate that CDI growth-inhibition pathways are distinct and can differ significantly even between closely related species.

Introduction

Contact-dependent growth inhibition (CDI) is a mechanism of inter-cellular competition used by some Gram-negative species to inhibit the growth of neighboring bacteria [1-3]. CDI is mediated by the CdiB/CdiA family of two-partner secretion proteins, which are distributed through α-, β- and γ-proteobacteria [4]. CdiB is an outer-membrane β-barrel protein that exports the CdiA toxic effector. CdiA proteins are very large (180 – 650 kDa depending on the species) and are predicted to form long β-helical filaments that extend from the surface of inhibitor cells [2,5]. During CDI, CdiA binds to specific receptors on susceptible bacteria and delivers a toxin domain derived from its C-terminal region (CdiA-CT). CdiA-CT sequences are highly variable between bacterial species and strains, but the N-terminal boundary of this region is typically delineated by a highly conserved VENN peptide motif [1,6]. CdiA-CT sequence diversity suggests a variety of toxin activities, and indeed most characterized CDI toxins are nucleases with different cleavage specificities for DNA, tRNA or rRNA [1,7-9]. Additionally, CdiA-CT^{EC93} from *Escherichia coli* EC93 appears to form pores in target-cell membranes [10], and sequence analysis suggests that other CDI toxins may have RNA deaminase and protease/peptidase activities [11]. CDI^{+} bacteria protect themselves from auto-inhibition by producing CdiI immunity proteins, which bind to CdiA-CT toxins and neutralize their activities.

CDI has been characterized most extensively in γ-proteobacteria, with *E. coli* EC93 and uropathogenic *E. coli* 536 (UPEC 536) serving as model systems. Studies with those systems have revealed that CDI exploits specific target-cell proteins to deliver growth inhibitory toxins [12,13]. Selections for mutants that are resistant to the *E. coli* EC93

system (CDI^{EC93}) identified *bamA* and *acrB* mutations that protect target cells from growth inhibition [12]. BamA is an essential outer-membrane protein required for the assembly of all β-barrel proteins [14-17], and is specifically recognized as a target-cell receptor by $CdiA^{EC93}$ [12,18]. AcrB is a trimeric integral membrane protein that functions together with AcrA and TolC as a multi-drug efflux pump [19]. However, the efflux function of AcrB is not required for CDI^{EC93} because Δ*acrA* and Δ*tolC* mutants are both fully sensitive to CDI^{EC93} [12]. Though the role of AcrB during CDI^{EC93} is not known, its localization suggests that it could facilitate assembly of the CdiA-CT^{EC93} pore-forming toxin into the target-cell inner membrane. Biochemical studies on CdiA-CT^{536} from UPEC 536 have shown that this toxin is a latent tRNase that only exhibits nuclease activity when bound to the cysteine synthase, CysK [13]. In accord with *in vitro* studies, *E. coli* Δ*cysK* mutants are completely resistant to inhibition by $CDI^{UPEC536}$. Collectively, these findings indicate that CDI pathways can encompass at least three distinct steps: i) receptor-binding to identify target bacteria, ii) translocation of CdiA-CT toxin across the target-cell envelope, and iii) activation of the toxin in the target-cell cytoplasm. Notably, the protective effects of *cysK* and *acrB* mutations are specific to the $CDI^{UPEC536}$ and CDI^{EC93} pathways, respectively [13]. These findings raise the possibility that each CDI system/toxin exploits a unique set of proteins to inhibit target-cell growth.

CdiB and CdiA share significant homology across the proteobacteria, but the CDI systems of Burkholderiales exhibit a number of differences compared to other bacteria. Firstly, the variable toxin region in *Burkholderia* CdiA is typically demarcated by the (E/Q)LYN peptide motif rather than the VENN sequence found in most other bacteria

[9,20]. *Burkholderia* toxins are modular and can be exchanged readily between *Burkholderia* CdiA proteins [9], but chimeric *E. coli* CdiA proteins carrying *Burkholderia* CdiA-CTs fused at the VENN sequence are not functional in CDI [1]. Secondly, CDI genes are arranged as *cdiAIB* clusters in *Burkholderia*, *Variovorax* and *Cupriavidus* species rather than the *cdiBAI* order found in other bacteria. This alternative gene arrangement is also correlated with a lack of "orphan" *cdiA-CT/cdiI* gene pairs. Orphan modules resemble the displaced 3′-fragments of full-length *cdiA* genes together with their cognate *cdiI* immunity genes [3,21]. Tandem arrays of orphan *cdiA-CT/cdiI* gene pairs are commonly found downstream of *cdiBAI* loci in γ-proteobacteria, and all strains of *Neisseria meningitidis* also carry well-defined orphan toxin/immunity clusters [21,22]. Finally, many *Burkholderia* CDI systems encode a small predicted lipoprotein, BcpO, between the *cdiI* and *cdiB* genes [20]. The function of BcpO is not understood completely, but it is required for CdiA secretion in *Burkholderia thailandensis* E264 [20]. Collectively, these observations suggest that the mechanisms of CDI in *Burkholderia* species are fundamentally distinct from other bacteria.

Here, we begin exploring *Burkholderia* CDI pathways using the $CDI_{II}^{Bp1026b}$ system encoded on chromosome II of *Burkholderia pseudomallei* 1026b as a model. We took a genetic approach and isolated transposon mutants of *B. thailandensis* E264 that are resistant to inhibition by the $CDI_{II}^{Bp1026b}$ system. Independent selections identified multiple transposon insertions in three genes – BTH_I0359, BTH_II0599 , and BTH_I0986, each of which confers resistance to $CDI_{II}^{Bp1026b}$. BTH_I0359 encodes a small cytosolic protein of unknown function, BTH_II0599 encodes an integral membrane

protein from the major facilitator superfamily (MFS), and BTH_I0986 encodes a predicted lipopolysaccharide (LPS) transglycosylase. We find that LPS structure is altered in BTH_I0986 mutants, suggesting that LPS may function as a receptor or co-receptor for $CdiA_{II}^{Bp1026b}$. These results demonstrate that the $CDI_{II}^{Bp1026b}$ is distinct from previously described *E. coli* pathways, suggesting that multiple pathways exist to translocate CDI toxins into target bacteria.

Materials and Methods

Bacterial strains and growth conditions

Bacterial strains were derived from *Burkholderia thailandensis* E264 and are listed in Table 1.1. Bacteria were routinely cultured in LB media supplemented with the following antibiotics where appropriate: kanamycin (Kan) 500 μg/mL; tetracycline (Tet) 25 μg/mL; trimethoprim (Tp) 100 μg/mL; chloramphenicol (Cam) 34 μg/mL; and polymyxin B (PB) 100 μg/mL. $CDI_{II}^{Bp1026b}$ competitions used Bt81 inhibitors, which are *B. thailandensis* E264 cells that express $cdiAIB_{II}^{Bp1026b}$ from plasmid pJSW1-6 (Table 1.2) [9]. Bt81 inhibitors and target cells were grown individually for at least 48 h (to $OD_{600} > 0.6$) in M9-minimal media supplemented with 0.2% L-arabinose. Approximately 10^9 colony-forming units (cfu) of Bt81 inhibitors and 10^8 cfu of target cells were mixed in 150 μL of M9-minimal medium supplemented with 0.2% arabinose, 1 μg/mL thiamine and 0.3 μg/mL ferric citrate, and aliquots plated onto LB agar supplemented with Tet or Kan to enumerate viable inhibitors and targets (respectively) at time 0 h. The remaining cell

mixture (100 μL) was spread onto M9-minimal medium agar supplemented with 0.2% L-arabinose, 1 μg/mL thiamine and 0.3 μg/mL ferric citrate and incubated for 24 h at 30 °C. Cells were then harvested from the agar surface, and viable inhibitor and target cell counts were determined as total cfu on Tet and Kan (respectively) supplemented LB agar. The competitive index (C.I.) was calculated as the ratio of target cells to inhibitor cells at 24 h divided by the target to inhibitor ratio at time 0 h. CDI^{E264} competitions were conducted in a similar manner, except inhibitor and target cells were co-cultured on tryptone broth agar. For these latter competitions, the target cells were derived from strain Bt36, which carries a deletion of the entire *cdiAIB*^{E264} gene cluster [9]. CdiA-$CT_{II}^{Bp1026b}$ toxicity was tested by expressing the toxin domain inside *B. thailandensis* cells. Plasmid pSCBAD-CTII1026b was introduced into *E. coli* DH5α and the resulting strain used in a four-parent mating with SM10λpir/pTNS3 [23,24], HB101 (pRK2013) [25] and *B. thailandensis* E264. Conjugation mixtures were split into two equal portions and plated on LB agar supplemented with PB, Tp and 0.2% D-glucose and LB agar supplemented with PB, Tp and 0.2% L-arabinose. The presence of exconjugants on plates supplemented with D-glucose and the simultaneous absence of exconjugant colonies after incubation at 37 °C for 48 h on the L-arabinose containing plates was indicative of toxicity.

Selection of CDI^R mutants

A library of random T23-Tp^R transposon-insertion mutants (>38,000 unique insertions) [26] was co-cultured with *B. thailandensis* Bt81 inhibitor cells [9]. Inhibitors and mutant target cells were mixed at a 10:1 ratio and plated onto M9 minimal agar medium supplemented with 0.2% L-arabinose 1 μg/mL thiamine and 0.3 μg/mL ferric citrate.

After 24 h co-culture at 37 °C, cells were harvested from the agar surface and surviving target cells isolated on Tp-supplemented LB agar. The target cells were pooled and subjected to two additional rounds of selection against $CDI_{II}^{Bp1026b}$ expressing inhibitor cells. After enrichment, individual clones were selected and tested for CDI-resistance in competition co-cultures with Bt81 inhibitor cells. Transposon-insertion junctions were amplified by arbitrary PCR using primers LacZ-124L2, LacZ-148 and CEKG 2E/K/L (Table 1.3). The resulting products were sequenced with primers LacZ211 and CEKG4 to identify insertion sites (Table 1.3).

Construction of plasmids and chromosomal deletions

Plasmid pSCBAD is a derivative of pSCRhaB2 [27]. The *araC* gene and *araBAD* promoter were excised from plasmid pCH450 [28] by NsiI/NcoI digestion and ligated to plasmid pSCRhaB2. This sub-cloning step replaces the original rhamnose-inducible promoter with an arabinose-inducible promoter. Plasmid pCH450 was amplified with primers CH1730/CH2799 and the resulting product cloned into pSCRhaB2 using NsiI/NcoI restriction sites to generate plasmid pSCBAD-KX. The BTH_II0599 and BTH_I0986 genes were amplified from chromosomal DNA using primers 3258/2725 and 3259/2729 (respectively), and the resulting products ligated to plasmid pSCBAD using EcoRI and XmaI restriction sites. BTH_I0359 was amplified using primers CH2059/CH2800 and ligated into pSCBAD-KX using KpnI and PstI restriction sites. The region encoding CdiA-$CT_{II}^{Bp1026b}$ (residues Met2821 – Asn3122 of full-length $CdiA_{II}^{Bp1026b}$) was subcloned from plasmid pCH450-CT_{II}^{1026b} [9] into pSCBAD using

NcoI and PstI restriction sites. The DsRed coding sequence was subcloned from plasmid pTrc-DsRed [8] into pSCBAD using NcoI and PstI restriction sites.

Gene deletions were constructed by allelic exchange as described previously [29]. DNA sequences upstream and downstream of the target gene were amplified and the two PCR products combined into one fragment using overlapping end PCR (OE-PCR) [30]. The OE-PCR products were ligated to plasmid pEX18-Tp (Table 1.2) using HindIII and KpnI/XbaI restriction sites. The BTH_I0359 deletion construct was generated using primer pairs 3296/3297 and 3298/3299; the BTH_II0599 deletion construct was generated using primer pairs 3182/3183 and 3184/3185; and the BTH_I0986 deletion construct generated using primer pairs 3103/3104 and 3105/3106 (Table 1.3).

Cell-cell adhesion

GFP-labeled *B. thailandensis* E264 [24] carrying plasmid pJSW1-6 (Bt121) or pJSW2 (Bt5) were grown overnight in tryptone broth, then diluted 1:50 in fresh tryptone broth and grown to OD_{600} ~0.5. DsRed-labeled target strains (Bt101, Bt123, Bt124 and Bt143) were grown in minimal M9-media supplemented with 0.2% L-arabinose for at least 48 h to OD_{600} ~ 0.5. Inhibitor and target cells were mixed at a 1:1 ratio and incubated for 30 min at room temperature to allow cell-cell binding. Cell suspensions were then diluted 1:50 into sterile filtered 1X phosphate buffered saline and analyzed by flow cytometry. Samples were run on an Accuri C6 flow cytometer using FL1 (533/30nm, GFP) and FL2 (585/40nm, DsRed) fluorophore filters. Cell-cell binding was measured as the percent of target cells in aggregates with inhibitor cells divided by the total number of target cells.

Binding data were normalized to the level of cell-cell binding between wild-type target cells (Bt101) and $CDI_{II}^{Bp1026b}$ expressing inhibitors (Bt121).

Lipopolysaccharide (LPS) analysis

Bacteria were grown to OD_{600} > 0.6 in M9-minimal medium supplemented with 0.2% L-arabinose and LPS was harvested from an equivalent of 10 mL of OD_{600} = 1 culture using the LPS Extraction Kit (Boca Scientific, USA). Purified LPS was resolved on a 4-20% polyacrylamide Tris-glycine SDS gel (Thermo Scientific) and visualized using ProQ 300 Emerald LPS stain (Molecular Probes, USA).

Results

Isolation of CDI^R mutants

To gain insight into the CDI pathways in *Burkholderia* species, we used a genetic approach to identify target-cell genes that are required for growth inhibition. We reasoned that mutants with disruptions in the genes encoding the CDI receptor, toxin translocators and toxin activators would be CDI-resistant (CDI^R). *B. thailandensis* E264 cells were subjected to random mutagenesis using a Tn*5*-based T23 transposon. Two independent T23 mutant pools were then co-cultured on solid media with *B. thailandensis* inhibitor cells that express the *B. pseudomallei* CDI_{II}^{Bp1026} system from a plasmid vector (Bt81, Table 1.1). CDI^R mutants were enriched through three cycles of co-culture with inhibitor bacteria, and 20 clones were selected for the identification of transposon insertion sites. Each mutant contained a T23 insertion within BTH_I0359,

BTH_II0599 or BTH_I0986; corresponding to eleven unique insertion sites (Fig. 1.1A & Table 1.1). BTH_I0359 is located upstream of the genes for methionine biosynthesis and encodes a hypothetical protein of 85 amino acid residues (Fig. 1.1A). BTH_II0599 encodes a predicted major facilitator superfamily (MFS) protein and is likely to be an inner-membrane localized transporter. BTH_I0986 is annotated as lipooligosaccharide (LOS) glycosyl-transferase G and is located within an LPS biosynthesis operon on chromosome I (Fig. 1.1A). We picked two mutants for each disrupted gene and confirmed that each was 10- to 100-fold more resistant to the CDI_{II}^{1026b} system than wild-type *B. thailandensis* (Fig. 1.1B).

Because multiple independent insertions were identified for each gene, it is likely that these mutations are directly responsible for the CDI^{R} phenotype. However, it is possible that the mutant strains carry additional unidentified mutations that contribute to resistance. To ascertain the roles of BTH_I0359, BTH_I0986 and BTH_II0599 in CDI, we constructed in-frame deletions of each gene and tested the resulting mutants for CDI^{R}. As expected, the deletion mutants each had CDI^{R} phenotypes that were very similar to the originally isolated transposon-insertion mutants (Figs. 1.1B & 1.2). ΔBTH_I0986 and ΔBTH_II0599 mutants were fully resistant to $CDI_{II}^{Bp1026b}$, whereas the ΔBTH_I0359 mutant was only partially protected from inhibition (Fig. 1.2). These results strongly suggest that each gene is required for the $CDI_{II}^{Bp1026b}$ inhibition pathway. We also showed that each deletion mutant was rendered sensitive to $CDI_{II}^{Bp1026b}$ when complemented with a plasmid-borne copy of the appropriate gene (Fig. 1.2). These latter

data exclude effects from transcriptional polarity and indicate that BTH_I0359, BTH_II0599 and BTH_I0986 are required for full sensitivity to the $CDI_{II}^{Bp1026b}$ system.

Resistance mutations are specific for the $CDI_{II}^{Bp1026b}$ system

B. thailandensis E264 carries its own CDI system (CDI^{E264}) and the $CdiA^{E264}$ protein shares approximately 53% sequence identity with $CdiA_{II}^{Bp1026b}$. However, the CdiA-CT^{E264} and CdiA-$CT_{II}^{Bp1026b}$ toxins are not homologous and have different nuclease activities [9], suggesting that the two toxin-delivery pathways could be distinct. Therefore, we asked whether mutations in BTH_I0359, BTH_II0599 and BTH_I0986 also provide resistance to CDI^{E264}. We first confirmed that Δ*cdiAIB*^{E264} mutants, which lack immunity to CDI^{E264}, are inhibited by wild-type CDI^{+} *B. thailandensis* cells as reported previously [9,20]. *B. thailandensis* Δ*cdiAIB*^{E264} targets were inhibited approximately 10^5-fold during co-culture with CDI^{+} cells (Fig. 1.3). This growth inhibition is attributable to CDI^{E264}, because the target cells were fully protected when complemented with the *cdiI*^{E264} gene on a Tn*7*-based vector (Fig. 1.3). We then introduced ΔBTH_I0359, ΔBTH_II0599 and ΔBTH_I0986 mutations into the Δ*cdiAIB*^{E264} background and found that each of the resulting strains was still sensitive to CDI^{E264} (Fig. 1.3). These results demonstrate mutations in BTH_I0359, BTH_II0599 and BTH_I0986 specifically confer resistance to the $CDI_{II}^{Bp1026b}$ system.

CDI^{R} genes are not required to activate the CdiA-$CT_{II}^{Bp1026b}$ toxin

Work with the CDI^{536} system from UPEC 536 has shown that some CDI toxins must be activated by so-called "permissive" factors. CdiA-CT^{536} only has tRNase activity when

bound to CysK, and therefore *E. coli* Δ*cysK* mutants are completely resistant to the toxin, even when produced at high levels inside the cell [13,31]. Based on the CDI^{536} paradigm, we asked whether any of the *Burkholderia* CDI^{R} genes encode proteins with permissive factor function. We placed the *cdiA-CT*$_{II}^{Bp1026b}$ coding sequence under control of an arabinose-inducible P_{BAD} promoter and moved the construct onto a mobilizable plasmid. This plasmid can be stably maintained in *E. coli* cells under conditions that repress transcription from P_{BAD} [9]. We then tested whether the *cdiA-CT*$_{II}^{Bp1026b}$ plasmid could be introduced into *B. thailandensis* cells through tri-parental mating. No exconjugants were produced from matings to introduce the toxin plasmid into wild-type cells, but dozens of exconjugants were obtained when recipient cells expressed the cognate *cdiI*$_{II}^{Bp1026b}$ immunity gene (Fig. 1.4). These results indicate that CdiA-CT$_{II}^{Bp1026b}$ is toxic when expressed inside *B. thailandensis* cells and that CdiI$_{II}^{Bp1026b}$ neutralizes the toxin to allow cell growth. We next performed matings with ΔBTH_I0359, ΔBTH_II0599 and ΔBTH_I0986 recipient strains, each of which produced no exconjugants (Fig. 1.4). Together, these results show that none of the CDI^{R} mutations protect the cell from intracellular CdiA-CT$_{II}^{Bp1026b}$, indicating that the corresponding gene products do not function as CDI permissive factors.

BTH_I0986 influences the binding of inhibitor and target cells

We next considered the possibility that the CDI^{R} genes may influence the recognition of target cells. The BTH_I0986 mutation is of particular interest because this gene belongs to the GT1 family of glycosyltransferases and is predicted to function in lipopolysaccharide (LPS) biosynthesis. Thus, the BTH_I0986 mutation could alter LPS

structure, thereby preventing $CDI_{II}^{Bp1026b}$ inhibitor cells from recognizing and/or binding to target bacteria. To determine whether BTH_I0986 influences LPS structure, we used SDS-PAGE to analyze LPS isolated from wild-type and ΔBTH_I0986 cells. Surprisingly, we found that LPS isolated from wild-type *B. thailandensis* E264 cells lacked polymeric O antigen (Fig. 1.5), in contrast to previous reports [32,33]. The LPS from ΔBTH_I0986 mutants also lacked an O-antigen ladder, but migrated more rapidly during electrophoresis than LPS from BTH_I0986^{+} cells (Fig. 1.5). Complementation with plasmid-borne BTH_I0968 restored mutant LPS to the wild-type mobility (Fig. 1.5). Therefore, disruption of BTH_I0986 alters the target-cell surface by changing LPS structure.

In the *E. coli* EC93 system, inhibitor cells bind stably to target bacteria and the resulting cell aggregates can be detected and quantified using flow cytometry [12,18]. Therefore, we used the same approach to examine the binding of $CDI_{II}^{Bp1026b}$ inhibitors to different target cell strains. We mixed GFP-labeled $CDI_{II}^{Bp1026b}$ inhibitors at a 1:1 ratio with DsRed-labeled target cells and analyzed the suspensions by flow cytometry to detect events with both green and red fluorescence, which correspond to aggregates containing both inhibitor and target cells. This analysis showed that approximately 40% more target cells bind to $CDI_{II}^{Bp1026b}$ inhibitors compared to CDI^{-} mock inhibitors (Fig. 1.6).

Discussion

The results presented here show that at least three genes, BTH_I0359, BTH_I0986 and BTH_II0599, are required for *B. thailandensis* cells to be fully inhibited by the

$CDI_{II}^{Bp1026b}$ system. We identified each gene in two independent selection experiments, suggesting that they represent the major non-essential genes required for the $CDI_{II}^{Bp1026b}$ pathway. Indeed, BTH_II0599 and BTH_I0986 are particularly critical because deletion of either gene provides full resistance to target bacteria. Notably, the three *B. thailandensis* genes identified here are distinct from those previously identified in *E. coli* within the CDI^{EC93} growth inhibition pathway [12]. These results suggest that the $CDI_{II}^{Bp1026b}$ and CDI^{EC93} systems deliver toxins through different pathways. CDI is initiated through direct binding interactions between CdiA and receptors on the surface of target bacteria. $CdiA^{EC93}$ uses the *E. coli* BamA protein as a receptor and appears to bind specific epitopes within extracellular loops eL6 and eL7 [12,18]. Our results here suggest that *B. pseudomallei* $CdiA_{II}^{Bp1026b}$ may exploit LPS as a target-cell receptor. BTH_I0986 is a predicted transglycosylase and mutants lacking this enzyme have altered LPS structure (Fig. 1.5). Moreover, the ΔBTH_I0986 mutant shows defects in binding to $CDI_{II}^{Bp1026b}$ inhibitor cells (Fig. 1.6), consistent with a role in receptor function. Surprisingly, we also found that our *B. thailandensis* E264 isolate lacks a detectable O-antigen ladder. This could account for the fact that we did not identify any additional LPS biosynthesis genes in independent selections. It is unclear whether the rough LPS phenotype reflects phase variation [34-36], or whether a rough-strain mutant was selected through laboratory passage. In either event, it will be important to determine how O-antigen influences CDI susceptibility in *Burkholderia* species. Although our results do not support a role for BamA in *Burkholderia* CDI, we acknowledge that CDI^{R} alleles of the essential *bamA* gene would be difficult to isolate using a transposon mutagenesis approach. If *Burkholderia* BamA does function as a CDI receptor, then the interactions

must be distinct from the CDI^{EC93} system, because BamA loops eL6 and eL7 loops differ significantly between *E. coli* and *Burkholderia* species (Fig. 1.7) [37].

Because CdiA-$CT_{II}^{Bp1026b}$ is a tRNase, this toxin must be transported into the target-cell cytoplasm to reach its substrate. CDI toxin translocation is poorly understood, but our recent work with *E. coli* indicates that transport across the target-cell outer membrane is energy-independent, whereas translocation into the cytoplasm requires the proton-motive force [38]. These findings raise the possibility that BTH_II0599, a predicted MFS transporter, is co-opted to translocate the tRNase domain across the target-cell inner membrane. In this model, periplasmic toxin would bind to BTH_II0599 and be driven into the cytoplasm by either the chemical or electrical potential of the pmf. These interactions are specific because the ΔBTH_II0599 mutation provides no protection against the *B. thailandensis* CDI^{E264} system, suggesting that the CdiA-CT^{E264} toxin must exploit another entry pathway. Although MFS proteins harness chemiosmotic gradients to transport a variety of metabolites [39,40], it seems unlikely that the transporter could translocate a folded nuclease domain in the same manner as small solutes. One possibility is that CdiA-CT_{II}^{Bp1026} has an autonomous membrane translocation activity, but requires BTH_II0599 as a receptor to facilitate insertion into the inner membrane. This model is similar to that proposed by Kleanthous and colleagues for the translocation of colicin nuclease domains, some of which interact with phospholipids and form pores in membranes [41-43].

The role of BTH_I0359 in the $CDI_{II}^{Bp1026b}$ pathway remains enigmatic, in part because the function of this gene is unknown. BTH_I0359 encodes a DUF3567 family member (PF12091, http://pfam.xfam.org/family/PF12091), which is only found within the order Burkholderiales. The gene neighborhood of BTH_I0359 includes the downstream $metH_a$ and $metH_b$ (which encode a split methionine synthase) and an upstream DUF3108 family member. DUF3567 and DUF3108 genes are linked throughout all the Burkholderiales, whereas linkage to *metH* is limited to *Burkholderia, Ralstonia* and *Cupriavidus* species. DUF3108 genes encode outer-membrane β-barrel proteins with a characteristic YmcC fold (PDB: 3FZX). Although strong genetic linkage is often indicative of a functional relationship, we did not isolate BTH_I0360 mutations in our CDI^R selections, even though this gene is not essential for *B. thailandensis* growth [26]. We have also excluded a "permissive" factor function for BTH_I0359. Permissive factors are target-cell proteins that are required to activate CdiA-CT toxins in the target-cell cytoplasm [13]. This conclusion is also supported by previous studies showing that purified $CdiA\text{-}CT_{II}^{Bp1026b}$ has tRNase activity *in vitro*, and therefore does not require an additional factor for activation [8].

All *B. pseudomallei* strains contain at least one CDI system, and some isolates carry up to three loci [9]. Each system can be placed into one of 10 different toxin/immunity groups [9,20], suggesting that CDI mediates competition between different *B. pseudomallei* strains. Using *B. thailandensis* as a model, Cotter and colleagues have recently demonstrated that such competition does in fact occur in mixed-strain biofilms, and that CDI influences the composition of these communities [20,44]. Additionally, there are

indications that *B. pseudomallei* and *B. thailandensis* do not co-inhabit the same environmental niches [45], again suggesting that anti-bacterial competition systems shape their environmental distributions. If *Burkholderia* species do in fact directly antagonize one another in the environment, then type VI secretion systems (T6SS) are more likely to effect this competition. *B. thailandensis* and *B. pseudomallei* strains all carry multiple T6SS, which have been shown to deploy toxins against both bacteria and eukaryotic targets [46-49]. Moreover, a given T6SS is capable of killing many different species of Gram-negative bacteria [50-52]. In contrast, CDI is a receptor-mediated process, and therefore variations in the cell-surface receptor epitopes restrict inhibition activity to a subset of bacteria [18]. In accord with this general model, data presented here show that CDI^{E264} is significantly more effective against *B. thailandensis* targets than $CDI_{II}^{Bp1026b}$. Together, these observations indicate that CDI is used primarily to differentiate sibling cells from other closely related bacteria.

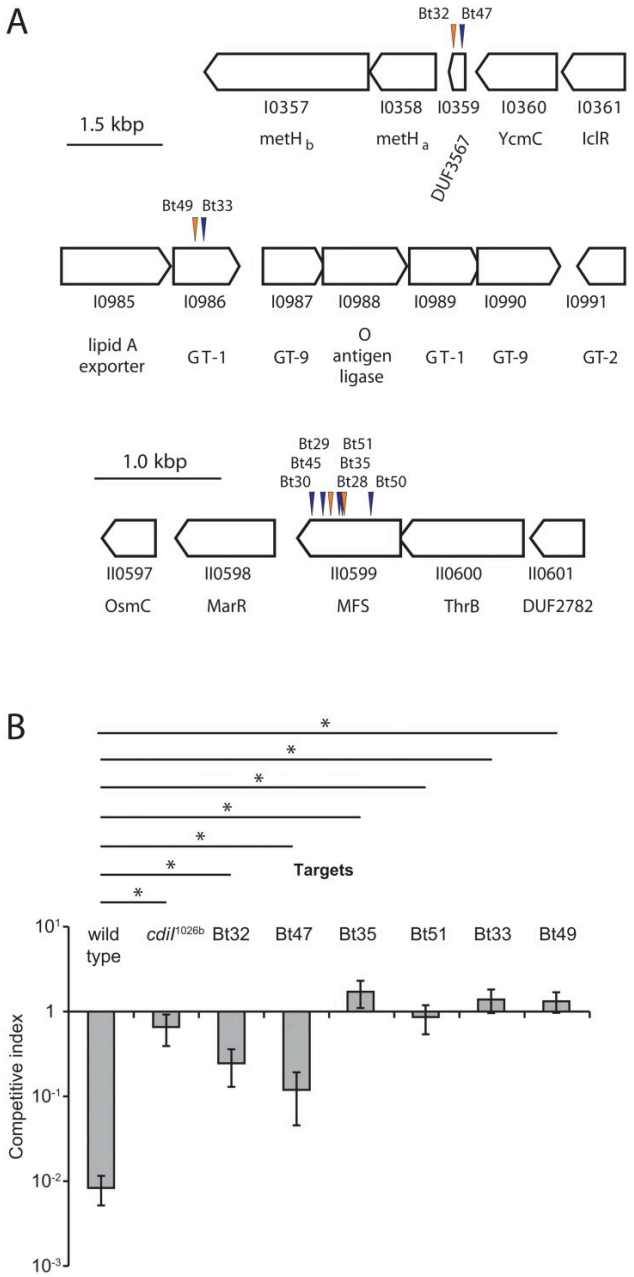

Figure 1.1. Selection of CDI^{R} mutants of B. thailandensis E264. (A) T23 transposon insertion sites were identified by semi-arbitrary PCR as described in Methods. Orange arrows indicate T23 insertions in the same transcriptional orientation of the disrupted gene and blue arrows indicate insertions in the opposite orientation. The corresponding CDI^{R} mutant strain number is given above each arrow. Automated gene annotations are given below each ordered locus designation. GT-1, GT-2 and GT-9 indicate predicted glycosyltransferase families and DUF designations indicate domains of unknown function. (B) The indicated *B. thailandensis* strains were co-cultured with Bt81 inhibitors (Table 1.1) that express the CDI$_{II}^{Bp1026b}$ system for 24 h on solid medium, and the competitive index was calculated as described in Materials and Methods. The strain labeled *cdiI*^{1026b} expresses the cognate CdiI$_{II}^{Bp1026b}$ immunity protein. Data represent the mean ± SEM for three independent experiments.

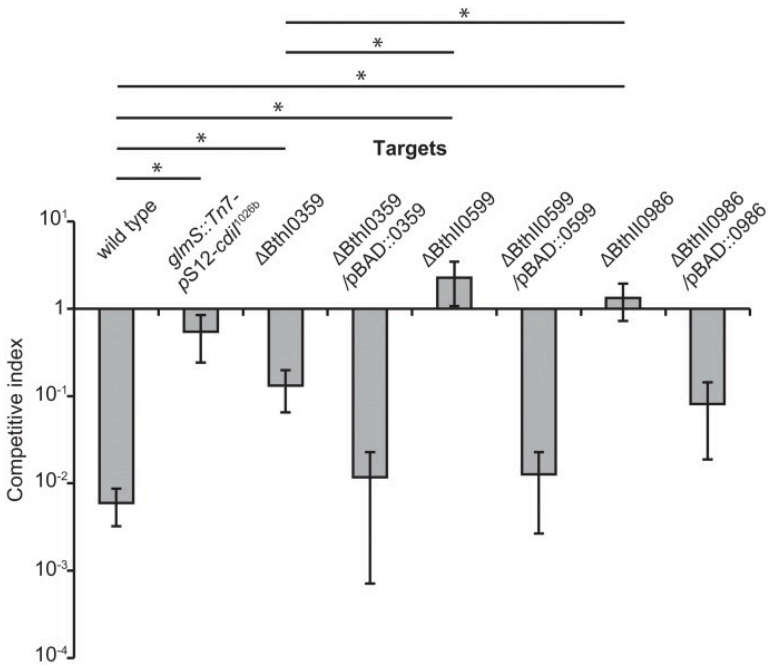

Figure 1.2. Complementation of CDI^{R} mutations. The indicated *B. thailandensis* strains were co-cultured with Bt81 inhibitors (Table 1.1) that express the $CDI_{II}^{Bp1026b}$ system for 24 h on solid medium, and the competitive index was calculated as described in Materials and Methods. The strain labeled *cdiI*^{1026b} expresses the cognate $CdiI_{II}^{Bp1026b}$ immunity protein. Plasmid-borne copies of BTH_I0359, BTH_I0986 and BTH_II0599 genes were expressed from an L-arabinose inducible promoter. Data represent the mean ± SEM for three independent experiments.

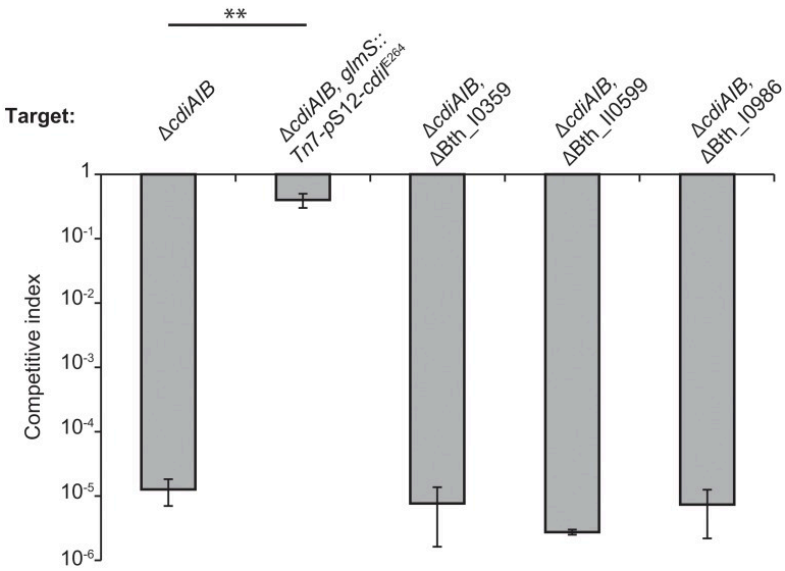

Figure 1.3. The CDI^{R} phenotype is specific for CDI$_{II}^{Bp1026b}$. The indicated *B. thailandensis* strains were co-cultured with wild-type (*cdiAIB*$^{+}$) *B. thailandensis* E264 cells for 24 h on solid medium, and the competitive index was calculated as described in Materials and Methods The strain labeled *cdiI*^{E264} expresses the cognate CdiI^{E264} immunity protein. Data represent the mean ± SEM for three independent experiments.

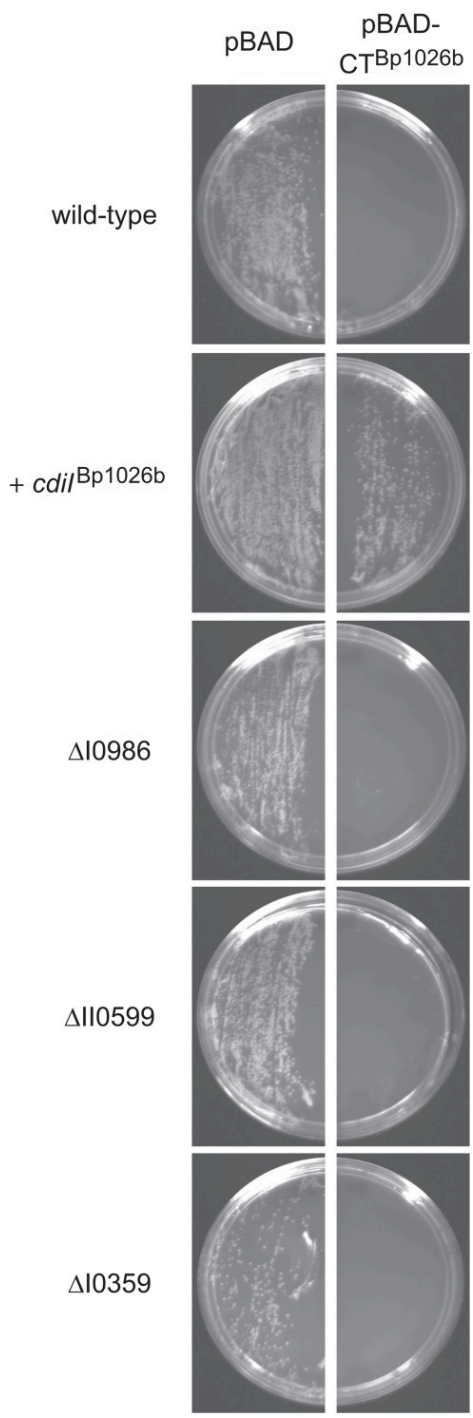

Figure 1.4. Toxicity of CdiA-CT$_{II}^{Bp1026b}$ expressed inside B. thailandensis cells. Plasmids pSCBAD and pSCBAD::*cdiA-CT*$_{II}^{Bp1026b}$ were introduced into the indicated *B. thailandensis* strains by conjugation as described in Materials and Methods. The mating mixtures were plated onto LB agar supplemented with L-arabinose and trimethoprim. The strain labeled *cdiI*$_{II}^{Bp1026b}$ expresses the cognate CdiI$_{II}^{Bp1026b}$ immunity protein.

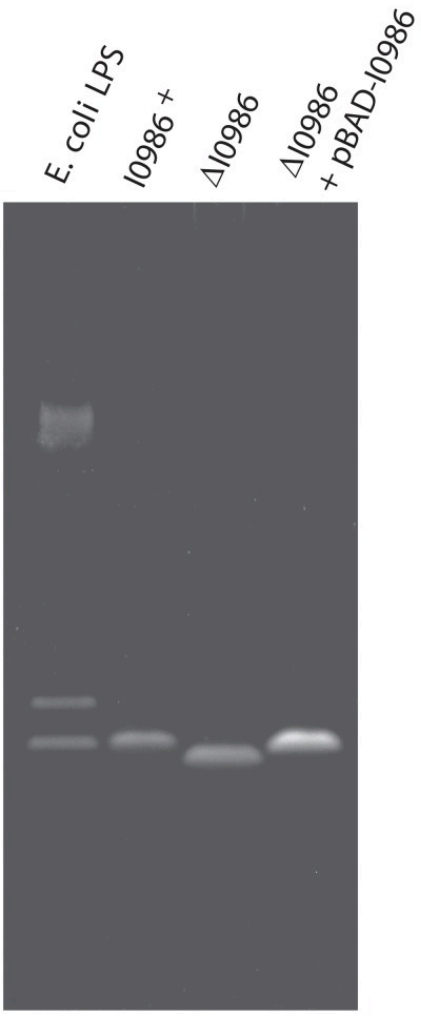

Figure 1.5. Lipopolysaccharide (LPS) analysis. LPS was isolated from the indicated *B. thailandensis* strains and analyzed by SDS-PAGE using fluorescent detection. The LPS standard is from *Escherichia coli* serotype 055:B5.

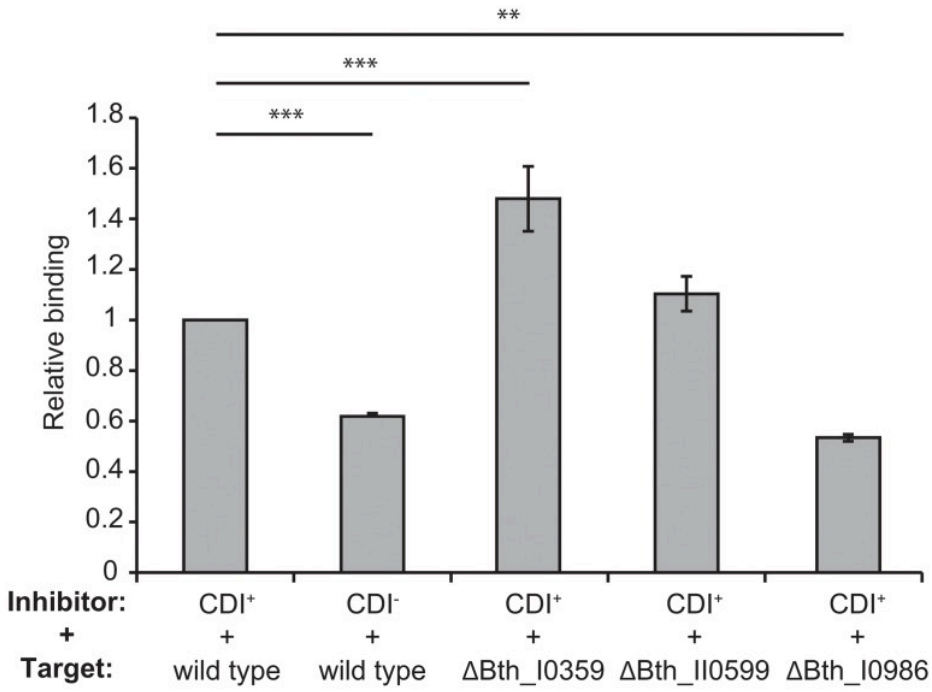

Figure 1.6. Cell-cell binding. CDI^+ (Bt81) and CDI^- (wild-type *B. thailandensis*) cells were labeled with GFP and mixed with the indicated DsRed-labeled target cells, then analyzed by flow cytometry to detect and quantify cell-cell aggregates. Binding was normalized to 1.0 for the interaction between Bt81 and wild-type *B. thailandensis* cells.

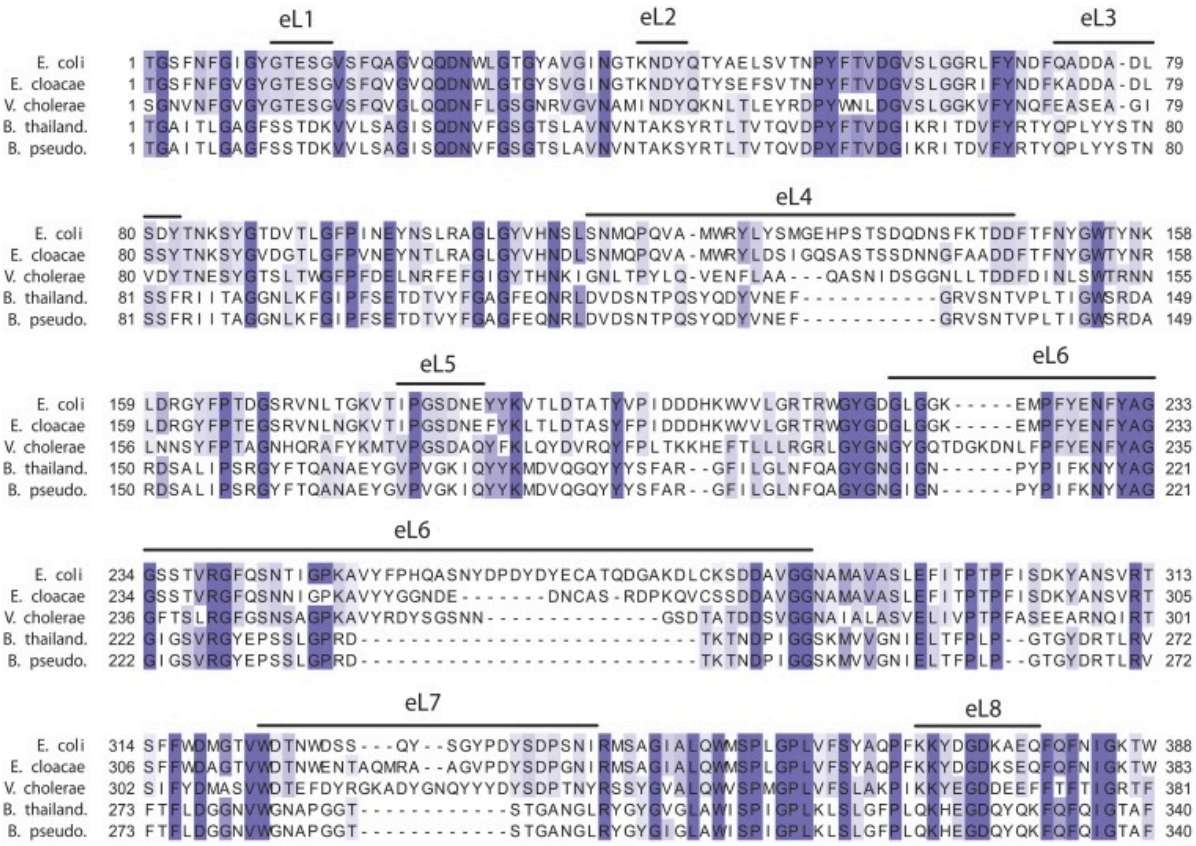

Figure 1.7. Alignment of BamA proteins. The β-barrel portion of BamA proteins from *E. coli* K-12 (Uniprot: P0A940), *Enterobacter cloacae* ATCC 13047 (D5CHY0), *Vibrio cholerae* ATCC 39315 (Q9KPW0), *B. thailandensis* E264 (Q2SWZ0) and *B. pseudomallei* 1026b (I1WHZ2). Sequences that correspond to extracellular loops (**eL**) are indicated above the alignment and are based on the crystal structures of BamA from *Neisseria gonorrhoeae and Haemophilus ducreyi* [37]. The alignment was rendered using Jalview 2.8 [55] at 30% sequence identity.

Table 1.1. Bacterial strains used in this study.

Strains	Description	Source or Reference
B. thailandensis E264	wild-type isolate	[54]
Bt5	*B. thailandensis* E264 (pJSW2)	This study
Bt6	*glmS1*::Tn7-Kan, Kan^R	[9]
Bt7	*glmS1*::Tn7-*cdiI*^{1026b}-Kan, Kan^R	[9]
Bt28	BTH_II0599::T23(IS*lacZ*-P*rhaB*o-FRT-Tp); T23 transposon inserted after nucleotide 557 of coding sequence, Tp^R	This study
Bt29	BTH_II0599::T23(IS*lacZ*-P*rhaB*o-FRT-Tp); T23 transposon inserted after nucleotide 611 of coding sequence, Tp^R	This study
Bt30	BTH_II0599::T23(IS*lacZ*-P*rhaB*o-FRT-Tp); T23 transposon inserted after nucleotide 720 of coding sequence, Tp^R	This study
Bt32	BTH_I0359::T23(IS*lacZ*-P*rhaB*o-FRT-Tp); T23 transposon inserted after nucleotide 226 of coding sequence, Tp^R	This study
Bt33	BTH_I0986::T23(IS*lacZ*-P*rhaB*o-FRT-Tp); T23 transposon inserted after nucleotide 514 of coding sequence, Tp^R	This study
Bt35	BTH_II0599::T23(IS*lacZ*-P*rhaB*o-FRT-Tp); T23 transposon inserted after nucleotide 524 of coding sequence, Tp^R	This study
Bt36	Δ*cdiAIB glmS1*::Tn*7*-*kan*, Kan^R	[9]
Bt45	BTH_II0599::T23(IS*lacZ*-P*rhaB*o-FRT-Tp); T23 transposon inserted after nucleotide 664 of coding sequence, Tp^R	This study
Bt47	BTH_I0359::T23(IS*lacZ*-P*rhaB*o-FRT-Tp); T23 transposon inserted after nucleotide 49 of coding sequence, Tp^R	This study
Bt49	BTH_I0986::T23(IS*lacZ*-P*rhaB*o-FRT-Tp); T23 transposon inserted after nucleotide 207 of coding sequence, Tp^R	This study
Bt50	BTH_II0599::T23(IS*lacZ*-P*rhaB*o-FRT-Tp); T23 transposon inserted after nucleotide 371 of coding sequence, Tp^R	This study
Bt51	BTH_II0599::T23(IS*lacZ*-P*rhaB*o-FRT-Tp); T23 transposon inserted after nucleotide 521 of coding sequence, Tp^R	This study

Bt56	Δ*cdiAIB glmS1*::Tn7-P_{rpsL}-*cdiI*^{E264}-*kan*, Kan^R	[9]
Bt79	*glmS1*::Tn7-P_{rpsL}-*gfp*-*kan*, Kan^R	T. Hoang
Bt81	pJSW1-6, Tet^R	[9]
Bt83	Δ*cdiAIB glmS1*::Tn*7*-*kan* ΔBTH_I0986, Kan^R	This study
Bt87	*glmS1*::Tn*7*-*kan* ΔBTH_II0599, Kan^R	This study
Bt101	*glmS1*::Tn*7*-*kan* pSCBAD::DsRed, Kan^R Tp^R	This study
Bt103	*glmS1*::Tn*7*-*kan* ΔBTH_I0986, Kan^R	This study
Bt104	Δ*cdiAIB glmS1*::Tn*7*-*kan* ΔBTH_II0599, Kan^R	This study
Bt111	*glmS1*::Tn*7*-*kan* ΔBTH_I0986 pSCBAD::I0986, Kan^R Tp^R	This study
Bt121	*glmS1*::Tn*7*-P_{rpsL}-*gfp*-*kan* pJSW1-6, Kan^R Tet^R	This study
Bt123	*glmS1*::Tn*7*-*kan* ΔBTH_I0986 pSCBAD::DsRed, Kan^R Tp^R	This study
Bt124	*glmS1*::Tn*7*-*kan* ΔBTH_II0599 pSCBAD::DsRed, Kan^R Tp^R	This study
Bt132	*glmS1*::Tn*7*-*kan* ΔBTH_I0359, Kan^R	This study
Bt134	Δ*cdiAIB glmS1*::Tn*7*-*kan* ΔBTH_I0359, Kan^R	This study
Bt137	*glmS1*::Tn*7*-*kan* ΔBTH_II0599 pSCBAD::II0599, Kan^R Tp^R	This study
Bt138	*glmS1*::Tn*7*-*kan* ΔBTH_I0359 pSCBAD::I0359, Kan^R Tp^R	This study
Bt143	*glmS1*::Tn*7*-*kan* ΔBTH_I0359 pSCBAD::DsRed, Kan^R Tp^R	This study

Abbreviations: Kan^R, kanamycin-resistant; Tet^R, tetracycline-resistant; Tp^R, trimethoprim-resistant

Table 1.2. Plasmids used in this study.

Plasmid	Description	Source or Reference
pEX18-Tp	Suicide vector containing *pheS** gene for *o*-chlorophenylalanine counter-selection, Tp^R	[55]
pSCRhaB2	Rhamnose-inducible promoter, Tp^R	[27]
pSCBAD	Derivative of pSCRhaB2 with *E. coli araC* and P_{BAD} promoter, Tp^R	This study
pSCBAD-KX	Derivative of pSCRhaB2 with *E. coli araC* and P_{BAD} promoter, Tp^R	This study
pJSW2	Shuttle vector carrying *oriVpVS1 oriVp15A oriT araC*-P_{BAD}, Tet^R	[9]
pJSW1-6	pJSW2-*cdiAIB*$_{II}^{1026b}$, expresses the *Bp* 1026b CDI_{II} system under control of the arabinose-inducible P_{BAD} promoter, Tet^R	[9]
pEX18-Tp:: ΔBTH_I0359	BTH_I0359 deletion construct, Tp^R	This study
pEX18-Tp:: ΔBTH_II0599	BTH_I0599 deletion construct, Tp^R	This study
pEX18-Tp:: ΔBTH_I0986	BTH_I0986 deletion construct, Tp^R	This study
pSCBAD-KX::0359	Arabinose-inducible expression of BTH_I0359, Tp^R	This study
pSCBAD::0599	Arabinose-inducible expression of BTH_I0599, Tp^R	This study
pSCBAD::0986	Arabinose-inducible expression of BTH_I0986, Tp^R	This study
pCH450-CT_{II}^{1026b}	Arabinose-inducible expression of residues Met2821 – Asn3122 of $CdiA_{II}^{Bp1026b}$, Tet^R	[9]
pSCBAD-CT_{II}^{1026b}	Arabinose-inducible expression of residues Met2821 – Asn3122 of $CdiA_{II}^{Bp1026b}$, Tp^R	This study
pTrc-DsRed	IPTG-inducible expression of DsRed, Amp^R	[8]
pSCBAD::DsRed	Arabinose-inducible expression of DsRed, Tp^R	This study

Abbreviations: Kan^R, kanamycin-resistant; Tet^R, tetracycline-resistant; Tp^R, trimethoprim-resistant

Table 1.3. Oligonucleotides used in this study.

Oligonucleotide	Sequence (Restriction endonuclease sites are in lowercase; N indicates equal mixture of all four deoxyribonucleotides)	Reference
2725	5′ - ATA Tcc cgg gTC ATC GAT CGG AGG TGT TCG	This study
2729	5′ - ATA Tcc cgg gTC ATC GCC CTC CGT TAC G	This study
3103	5′ - CAA CAA aag ctt CAT CGA CAC GCT CGT GGG AGA	This study
3104	5′ - GAT CGT ACT GGA TCG CTGC ACG CCA AAA ACC AAC GGC CGG ACC C	This study
3105	5′ - GCG TGC AGC GAT CCA GTA CGA TC	This study
3106	5′ - CAA CAA ggt acc CGT GTC GCC GAG CAA CAG ATG A	This study
3182	5′ - CAA CAA aag ctt CAT CAG CCG AAC CTG CGC AGC	This study
3183	5′ - GAT CGG AGG TGT TCG GCA GCT TCG CGG AAC CAC ACG TAG CCG G	This study
3184	5′ - GAA GCT GCC GAA CAC CTC CGA TC	This study
3185	5′ - CAA CAA ggt acc GAG CAG CGG CTT GTA CGC CTT	This study
3258	5′ - GCG Cga att cCG AGA CCC ACG CAT GCA AC	This study
3259	5′ - GCG Cga att cCA GGG CGC CAT TCG ATG AC	This study
3296	5′ - ATA Taa gct tCT GCG TGA TCG ACA AGA GC	This study
3297	5′ - CCG CCA TGC AAA TGA TCT ACA ACC CGT CGT TCT CCA CTG	This study
3298	5′ - CAG TGG AGA ACG ACG GGT TGT AGA TCA TTT GCA TGG CGG	This study
3299	5′ - GCG Ctc tag aGA TCG GCG ACG AAA CGA TCT	This study
CH1730	5′ - GTA cca tgg TAC CTT CCT CCT GCT AGC	This study
CH2059	5′ - AGT ggt acc ATG CAA ATG ATC TAC AAC AGC	This study
CH2799	5′ - GAT atg cat AAT GTG CCT GTC AAA TGG	This study
CH2800	5′ - TAC TGC AGC CCT CGA GTC AGT GGA GAA CGA CG	This study
LacZ-124L2	5′ - CAG TCA CGA CGT TGT AAA ACG ACG	This study
LacZ-148	5′ - GGG TAA CGC CAG GTT TTT CC	This study
LacZ-211	5′ - TGC GGG CCT CTT CGC TAT TA	This study
CEKG 2E	5′ - GGC CAC GCT CGA CTA GTA CNN NNN NNN NNA TGT A	This study
CEKG 2K	5′ - GGC CAC GCG TCG ACT AGT ACN NNN NNN NNN AGT GC	This study
CEKG 2L	5′ - GGC CAC GCG TCG ACT ACN NNN NNN NNN CTG AG	This study
CEKG 4	5′ - GGC CAC GCG TCG ACT AGT AC	This study

Chapter 2

Identification of BamA residues critical for interaction with CdiA^{EC93}

Abstract

Contact-dependent growth inhibition (CDI) was initially discovered in a rat intestinal isolate, *Escherichia coli* EC93, that inhibited the growth of other *E. coli* strains. The CDI system of EC93 uses the outer membrane β-barrel protein BamA as an outer membrane receptor to recognize and bind target cells. $CdiA^{EC93}$ interacts with the extracellular loops 4, 6, and 7 of BamA, but the mechanism by which CdiA-CT toxins enter the cell has remained unclear. I have identified specific amino acids in BamA loops 4 and 6 that are necessary for binding and inhibition by $CdiA^{EC93}$. I isolated mutations in these loops that affect residues in a small pocket-like surface-exposed region of BamA. The mutations confer full resistance to CDI^{EC93} and prevent inhibitors expressing $CdiA^{EC93}$ from binding, but do not result in any growth defects. By narrowing down the BamA-$CdiA^{EC93}$ interaction to a key binding pocket, these findings further our understanding of the molecular mechanisms underlying toxin delivery to sibling cells.

Introduction

Contact-dependent growth inhibition (CDI) is a mechanism by which Gram-negative bacteria touch and then deliver toxins into neighboring cells [1-3]. Sibling cells are immune to the toxin due to expression of a small immunity protein known as CdiI, whereas growth of "non-self" cells is blocked by activity of the toxins, which include DNases, RNases, and pore-formers [1,7-9]. CDI has been most extensively characterized in *Escherichia coli* EC93 [2,10,12,18,21,56]. The outer membrane protein BamA was identified as the receptor for $CdiA^{EC93}$ based on the finding that a transposon insertion

immediately upstream of *bamA* conferred partial resistance to CDI^{EC93} by decreasing BamA surface levels about five-fold [12].

BamA is an essential outer membrane protein (OMP) of the Omp85 superfamily, and the core member of the β-barrel assembly machinery (BAM) complex, which is required for proper folding and membrane insertion of almost all β-barrel OMPs [14-17,57-58]. In addition to BamA, the BAM complex contains the accessory lipoproteins BamB, BamC, BamD, and BamE, which are anchored in the inner leaflet of the outer membrane [59]; none of these lipoproteins appear to participate in the CDI^{EC93} pathway [12].

Crystal structures of BamA and the related protein FhaC indicate that it consists of a 16-stranded transmembrane β-barrel domain, 5 periplasmic polypeptide translocation-associated (POTRA) domains, and a series of variable extracellular loops [37,59-62]. Loops 4, 6, and 7 together form a cap or dome over the barrel that is stabilized by a salt bridge interaction between residues R547 (loop 4), E645 (loop 6), and D746 (loop 7) [57,60]. Loop 4 contains a structurally conserved α-helix that sits parallel to the membrane and is essential for cell survival [37,60]. Loop 6 forms a hairpin tucked inside the β-barrel, with a highly conserved (V/I)RG(F/Y) motif at the tip which is critical for assembly of substrate OMPs [57,65-67].

BamA is also the outer membrane receptor for Shiga toxin-encoding bacteriophages (Stx phages), which are responsible for the evolution of Shiga toxin-encoding *E. coli* pathogens, including serotype O157:H7 [63]. Stx phage also use regions of loops 4, 6,

and 7 for adsorption, which may explain their limited host range [63]. It was recently reported that the envelope stress response triggered by Stx phage adsorption leads to decreased *bamA* expression, presumably as a defense mechanism against further invasion [64]. Interestingly, CDI^{EC93} also induces the *pspA* (phage shock) transcription response, though this response is not necessary for inhibition [10].

The high sequence variability of the extracellular loops restricts the target range of CDI systems to closely related cells (Fig. 1.7). We have previously reported that CDI^{EC93} requires $BamA^{Ecoli}$ extracellular loops 4, 6, and 7 for inhibition [18]. Mutations in loops 6 and 7 abolish inhibitor-target binding and are presumed to be necessary for target cell recognition. Deletion of a polymorphic region of loop 4 (not containing the α-helix) confers partial resistance to CDI^{EC93} and has a minor impact on cell-cell binding, leaving the role of loop 4 in CDI delivery unclear [18].

We have previously characterized several CDI systems by constructing cosmid-borne chimeric CDI systems, which consist of the N-terminal region of $CdiA^{EC93}$ fused at the VENN motif to the CdiA-CT/CdiI toxin/immunity modules from other strains [7-9,21,68-69]. This facilitates use of *E. coli* as a model system, as the N-terminal region of $CdiA^{EC93}$ contains the binding site for BamA and ensures that the toxin is delivered [1]. In an attempt to investigate the CDI pathway of *Enterobacter cloacae* (ECL), we used an EC93-ECL chimeric CDI system to select for targets resistant to $CdiA\text{-}CT^{ECL}$ [7]. We did not successfully identify any target cell factors specific to *E. cloacae*, which may be

explained by the fact that CdiA-CT^{ECL} interacts with ribosomal RNA [7]. However, we did identify several mutations in the coding sequence of *bamA*.

Here, I further explore the interactions between CdiA^{EC93} and BamA^{Ecoli} in order to better understand binding and delivery of CDI toxins. I isolated a series of deletion and point mutations that confer resistance to the EC93-ECL chimeric CDI system. These mutations affected the conserved α-helix in loop 4 and the unconserved Phe^{675} of loop 6, but did not cause any observable growth defects. Strikingly, point mutations in both loops completely abolished inhibitor-target binding. These results, when compared to recent crystal structures of BamA, suggest that a unique CdiA^{EC93} binding site is shaped by both polymorphic and conserved features of BamA extracellular loops.

Materials and Methods

Bacterial strains and growth conditions

Strains are listed in Table 2.1; plasmids are listed in Table 2.2; and oligonucleotides are listed in Table 2.3. Strains were grown in Luria Broth (LB) or Tryptone Broth (TB) media. Antibiotics were used at the following concentrations: ampicillin (Amp) 100μg/ml; chloramphenicol (Cm) 34 μg/ml; kanamycin (Kan) 40μg/ml. Cultures were incubated at 37˚C in an environmental shaker apparatus at 226rpm unless otherwise indicated.

Ultraviolet light (UV) mutagenesis

Overnight bacterial cultures were diluted 1:100 in 100 mL LB agar supplemented with Kan and grown to OD_{600} = 0.4. Cells were harvested by centrifugation in 50mL Falcon tubes at 3500 rpm for 15 minutes, resuspended in 50 mL 0.1M $MgSO_4$, and incubated on ice for 5 minutes. Cells were irradiated with 32 mJ/m^2 of UV using the Stratalinker 1800, immediately transferred to light-blocking 50mL Falcon tubes to prevent photoreactivation, and centrifuged at 3500rpm for 15 minutes at 4˚C. The cell pellet was resuspended in 25ml LB supplemented with Kan, transferred to 250ml baffled flasks wrapped in aluminum foil, and incubated overnight. Mutant pools were subjected to three rounds of growth competition as described below against *E. coli* strain DL8680 to enrich for CDI resistance.

Growth competition assays

Overnight cultures of CDI+ inhibitor cells were diluted 1:100 in LB and grown to 0.4-0.45 OD_{600} in a baffled flask. Inhibitors and targets were mixed at a 1:1 ratio and incubated in 5ml LB in a baffled flask at 37˚C for 3 hours. Serial dilutions were plated at 0 hours and 3 hours on LB with relevant antibiotics to distinguish inhibitors from targets (Figure 2.3A).

Selection of CDI^R mutants

Pools of UV mutants were prepared as described above from *E. coli* DL5562 (Table 2.2). Each bacterial pool was subjected to a growth competition assay against DL8680 inhibitor cells and surviving target cells were isolated on LB agar supplemented with

Kan. The target cells were pooled and subjected to two additional rounds of selection against DL8680. Individual clones were then tested for CDI-resistance in a competition assay against DL8680. To establish whether *bamA* mutations were responsible for the CDI-resistance phenotype, mutants were transformed with the complementation vector pZS21-*bamA*-amp and tested for CDI-sensitivity against DL8680. The *bamA* sequence of *bamA* mutant strains was determined following PCR and sequencing with a series of three oligonucleotide pairs that together gave full coverage of the *bamA* gene. Oligonucleotides 1157 and 3939 were used to amplify the *bamA* regulatory region and first 1000bp of *bamA*, sequenced using oligonucleotide 1168. Oligonucleotides 3691 and 3938 were used to amplify the central 1000bp of *bamA*, sequenced using oligonucleotide 3937. Oligonucleotides 2586 and 2587 were used to amplify the terminal 1000bp of *bamA*, sequenced using oligonucleotide 2462 (Table 2.4).

Quick transformation

Quick transformation was performed as previously described [70]. Cells were grown to OD_{600} ~0.4 and mixed with 50µl ice cold LB broth and and 50µl 2x TSS (1x TSS: LB broth, 10% wt/vol polyethylene glycol, 51% vol/vol dimethylsulfoxide, and 50mM Mg^{2+}, pH 6.5). ~100ng of plasmid prep was added and the mixture was incubated on ice for 30-60 minutes. Following ice incubation, 0.9mL 1x TSS 20mM glucose was added and cells were incubated for 1-2 hours at 37˚C with shaking, then plated on LB agar supplemented with appropriate antibiotics.

Preparation of electrocompetent cells

Overnight cultures were diluted 1:100 in 50ml LB, grown to OD_{600} ~0.4 in a baffled flask and placed on ice for 5 minutes, then transferred to a chilled 50ml Falcon tube and centrifuged at 6000rpm for 10 minutes at 4˚C. Cells were resuspended in 50ml ice cold sterile water and centrifuged again at 6000rpm for 10 minutes at 4˚C. This step was repeated, then cells were resuspended in 5ml ice cold 10% glycerol and centrifuged at 10000rpm for 5 minutes at 4˚C. Cells were resuspended in 0.75ml ice cold 10% glycerol, and 50µl aliquoted into Eppendorf tubes and stored at -80˚C until electroporation.

Introducing bamA mutations into pZS21-bamA

To excise the wild-type *bamA* allele from pZS21-*bamA*-kan, the plasmid was digested with restriction enzymes EcoRI and XbaI and analyzed on a 1% agarose gel containing GelStar™ Nucleic Acid Gel Stain (Lonza) to resolve *bamA* from the vector backbone. The vector backbone DNA (3.6kb) was purified by QIAex Gel Extraction Kit (QIAGEN). Mutant *bamA* alleles were amplified from mutant genomic DNA using oligonucleotides 3953 and 3954, digested with EcoRI and XbaI in CutSmart® buffer, and ligated with the pZS21-kan gel extraction product using T4 ligase. The ligation was electroporated into EPI100 electrocompetent cells, plated on LB supplemented with Kan, and incubated overnight. Plasmid DNA of resulting transformants were checked for presence of insert by running a double restriction digest (EcoRI and XbaI) of the plasmid prep on an ethidium bromide 1% agarose gel. The presence of loop 4 mutations was verified by sequencing plasmid DNA with oligonucleotide 3937; the presence of loop 6

mutations was verified by sequencing plasmid DNA with oligonucleotide 2462 (Table 2.4).

Plasmid exchange

Plasmid exchange of pZS21-*bamA* was performed as previously described [18]. Briefly, DL6917 containing plasmid pZS21-*bamA*-amp was prepared for electroporation as described above. Electrocompetent cells were transformed with pZS21-*bamA*-kan derivatives carrying mutant *bamA* alleles, plated on LB agar supplemented with Kan, and incubated overnight. Kan^R colonies were patched onto LB agar plates supplemented with Amp or Kan and incubated overnight to ensure Amp sensitivity and Kan resistance.

Growth curves

Overnight cultures were back-diluted to OD_{600} 0.025 in LB in a baffled flask and incubated at 37˚C for 4 hours. 1mL of culture was removed every 30 minutes to measure OD_{600}.

Binding assays

Cell-cell binding assays were performed essentially as previously described [18] Briefly, overnight cultures of CDI^+ inhibitors (DL4905 and DL4906, Table 2.2) were grown in TB supplemented with Amp at 30˚C with shaking, and overnight cultures of target cells containing pZS21-*bamA* and pDsRedExpress2 (Table 2.3) were grown in LB supplemented with Amp and Kan at 37˚C with shaking. CDI^+ inhibitor cells were diluted 1:100 in filtered TB supplemented with Amp and Kan in a non-baffled flask and grown

to OD_{600} ~0.5 at 30˚C with shaking. Inhibitors and targets were mixed at a 4:1 ratio in filtered TB for a final OD_{600} 0.2, grown for 15 minutes at 30˚C with shaking, and diluted 1:100 in PBS. Cell-cell binding was analyzed with the Accuri C6 flow cytometer using FL1 (533/30 nm, GFP) and FL2 (585/40 nm, DS-Red) fluorophore filters (Becton Dickinson).

Results

Isolation of bamA CDI^R mutants

The initial goal of this project was to identify the target-cell genes necessary for growth inhibition by CDI^{ECL}. I constructed a pool of *mariner*-transposon insertion mutants [71] from DL5564 to use in a growth competition assay (Fig. 2.3A) against CDI+ *E. coli* inhibitor cells expressing the EC93-ECL chimeric CDI system (DL8680, Table 2.2). CDI^R mutants were enriched through three rounds of selection against DL8680. Only one of the pools enriched through all three rounds, and 10 clones from this pool were selected for the identification of transposon insertion sites. The mutants contained an insertion upstream of the uncharacterized gene *yjfY*, but when the mutation was transduced into a fresh background, cells were no longer resistant to DL8680 (data not shown). This suggested that another mutation conferring resistance to DL8680 was present, and that the transposon insertion in *yjfY* was not linked to the CDI^R phenotype. I theorized that the mutation may lie in *bamA* because the EC93-ECL chimeric CdiA contains the BamA binding site and targets BamA as its outer membrane receptor. To determine whether

CDI resistance was due to a mutation in *bamA*, cells were transformed with the plasmid pZS21-*bamA*-amp, which expresses wild-type $bamA^{Ecoli}$ (Table 2.3). Complementation with wild-type $bamA^{Ecoli}$ restored sensitivity to DL8680, and the *bamA* gene of the 10 clones was sequenced. All were found to contain ΔA672_N681, a 10-residue deletion in the surface-exposed region of loop 6 (Figs. 2.1 & 2.2, Table 2.1).

$CdiA\text{-}CT^{ECL}$ is a ribosomal RNase, and may interact with essential proteins, making it difficult to isolate CDI^R mutants by transposon mutagenesis, which generally ablates gene function. Therefore we simultaneously took a UV mutagenesis approach to induce point mutations in the *E. coli* genome. DL5562 target cells were mutagenized by UV, and CDI^R mutants were enriched through three rounds of selection against DL8680. 7 independent mutant pools enriched, and individual clones from each pool were quick-transformed with pZS21-*bamA*-amp to determine whether CDI resistance was linked to *bamA* mutations. All 7 clones tested became sensitive to DL8680 when complemented with pZS21-*bamA*-amp, and the *bamA* gene from each clone was sequenced. 4 additional mutations were identified in the surface-exposed region of loop 6, all affecting the same phenylalanine residue: ΔF675 (isolated twice), F675C, F675C/P676L, and F675Y/P676S. 2 mutations were identified in the α-helical region of loop 4: V543N/W546C and ΔR547/Y548H (Figs. 2.1 & 2.2, Table 2.1). All mutations conferred full resistance to CDI (Figs. 2.3B & C, 2.4B & C).

I selected 3 CDI^R mutants to study further: V543N/W546C, ΔA672_N681, and ΔF675. The mutant *bamA* alleles were moved into an *E. coli bamA::cat* background to facilitate

cell-cell binding assays. The *bamA* alleles from each mutant were amplified from genomic DNA and used to replace the wild-type *bamA* allele in pZS21-*bamA*-kan (Fig. 2.5A, Table 2.3). The plasmids carrying mutant *bamA* alleles were transferred by plasmid exchange into an *E. coli bamA::cat* background, generating the strains DL8807, DL8804, and DL8805, which express only the V543N/W546C, ΔA672_N681, and ΔF675 mutant *bamA* alleles respectively (Table 2.2). These strains also exhibited full resistance to DL8680 inhibitors (Fig. 2.5B).

The bamA CDI^R mutants do not exhibit growth rate defects

Although BamA is an essential protein, we have previously shown that portions of loops 4 and 6 can be deleted with no detectable growth defects [18]. However, the region of loop 4 that was deleted did not contain the structurally conserved α-helix [18]. It has recently been reported that an R547A mutation in the α-helix of loop 4 is lethal, presumably by disrupting a stabilizing salt-bridge interaction with residues E645 in loop 6 and D746 in loop 7 [60]. We isolated a nonlethal mutation affecting the same arginine residue (ΔR547/Y548H), but wondered whether the mutant exhibited growth defects. I assessed cell viability through log phase by performing growth curves over a period of 4 hours. The ΔR547/Y548H mutant grew normally, suggesting that, unlike alanine, the slightly basic side chain of histidine can still form a functional salt bridge (Fig. 2.6A). The only mutant with a distinct growth defect was DL8738, or ΔF675 (I) (Fig. 2.6B). However, because the other ΔF675 mutant (DL8830) grew normally, DL8738 is presumed to have an additional mutation elsewhere in the chromosome that is responsible for the growth rate phenotype. This is supported by the fact that *E. coli bamA::cat*

pZS21-*bamA*$^{\Delta F675}$-kan cells also grew normally. Therefore, the loop 4 and loop 6 mutations isolated in our screen do not appear to have a discernable effect on cell viability or growth rate.

The bamA CDI^{R} mutations block binding between targets and inhibitors

Previous work has shown that mutations in loops 4, 6, and 7 of BamA confer CDI^{EC93} resistance and disrupt binding between targets and inhibitors. Specifically, a ΔF675_S702 mutation in loop 6 and an HA tag in loop 7 both confer full CDI^{EC93} resistance and completely abrogate binding, while a ΔP556_S564 mutation in loop 4 leads to a modest decrease in binding and increase in resistance [18]. This deletion does not overlap with the mutations we found in the loop 4 α-helix (Fig. 2.1, Table 2.1). I sought to determine whether the *bamA* mutations isolated in this screen conferred CDI resistance by blocking cell-cell binding. GFP-labeled *E. coli* inhibitors expressing the full EC93 system were mixed with DsRed-labeled targets expressing *bamA* from the plasmid pZS21-*bamA*-kan (Tables 2.2 & 2.3). After a short co-culturing period, the cell mixtures were analyzed by flow cytometry to detect inhibitor-target aggregates, which emit both a green and red fluorescent signal (Fig. 2.7A). The ΔA672_N681, ΔF675, and V543N/W546C mutants all failed to aggregate with inhibitor cells, at a rate similar to targets expressing *bamA*^{ECL}, which cannot bind CdiA^{EC93} (Fig. 2.7B) [18]. These data indicate that single point mutations in loops 4 and 6 are sufficient to abrogate cell-cell binding.

Discussion

The results presented here show that BamA in *E. coli* contains several specific residues necessary for binding by $CdiA^{EC93}$. We identified mutations in extracellular loops 4 and 6 which confer full resistance to CDI by blocking cell-cell binding, yet have no effect on cell growth. Five unique mutations affected F675 in loop 6, among them a single amino acid deletion and a single substitution (Table 2.1). F675 is not conserved in other species, which agrees with previous findings that $CdiA^{EC93}$ only interacts with $BamA^{Ecoli}$ (Fig. 1.7) [18]. The two mutations found in the loop 4 α-helix are more enigmatic. The loop 4 α-helix is structurally conserved in BamA homologs, and the amino acid sequence of the helix is nearly identical between *E. coli* and *Enterobacter cloacae* [37]. However, $CdiA^{EC93}$ is unable to bind $BamA^{ECL}$, suggesting that the loop 4 α-helix itself is insufficient for cell-cell binding and inhibition [18]. Together, these discoveries indicate that loops 4 and 6 help to form a binding epitope for $CdiA^{EC93}$.

BamA was initially identified as the outer membrane receptor for $CdiA^{EC93}$ based on the analysis of a transposon-induced mutation in the *bamA* regulatory region that rendered cells resistant to CDI [2]. Because this mutation (*bamA101*) did not affect the structure of BamA, but instead decreased BamA surface levels, *bamA101* mutants did not exhibit the degree of CDI resistance observed in cells provided with *bamA* alleles from other species [18]. The mutations isolated in this study permit a closer look at the precise molecular interactions between BamA and $CdiA^{EC93}$.

According to a recent crystal structure of BamA, F675 and the loop 4 α-helix are located in immediate proximity to one another (Fig. 2.2) [60]. These and several nearby residues from loops 4, 6, and 7 appear to form a small indentation or pocket in the dome over the barrel (Fig. 2.2). Work from our lab has shown that a 7-HA tag that replaces Y754_S755 with an HA epitope completely abrogates binding and confers CDI resistance [18]. Examination of the crystal structure of BamA shows that Y754 is immediately adjacent to F675 and the loop 4 α-helix (Fig. 2.2), supporting the hypothesis that this pocket on the surface of BamA acts as the $CdiA^{EC93}$ binding epitope. Before the publication of the BamA crystal structure discussed above, it was found that deleting P556_S564 of loop 4 results in a modest increase in resistance and decrease in binding [18]; a possible mechanism for this phenotype is that shortening loop 4 adjusts the position of the α-helix and alters the conformation of the binding pocket. Performing a mutant screen of other residues in the binding pocket, as well as other members of the α-helix, would be a key component of future studies. This would also facilitate the identification of the BamA binding site on CdiA, perhaps by performing a screen for *cdiA* mutations that suppress the *bamA* mutations from this study.

The mechanism(s) by which CDI toxins cross the outer membrane is not yet understood. Current knowledge of BamA structure and function suggests a few potential mechanisms of toxin entry. Colicins bind first to one outer membrane receptor and then enter through another [72] though if this were the case for $CdiA^{EC93}$, a second receptor would presumably have been discovered in previous screens for CDI^{R} mutants. The β-barrel domain of BamA is sufficient to cause local membrane destabilization [73], and it is

possible that CDI toxins utilize the destabilized membrane region surrounding BamA to "sneak" through the outer membrane.

Analysis using engineered disulfide bridges revealed that the β-barrel also contains a lateral opening and exit pore through which substrate OMPs are predicted to move into the outer membrane [66]; this is another potential site for CdiA-CT entry. The crosslinked BamA mutants engineered by Noinaj and colleagues [66] could be used to test whether CDI requires either pore opening or lateral β-barrel opening for delivery. Although these crosslinked mutants are lethal, we can circumvent this by supplying cells with another *bamA* allele which does not bind $CdiA^{EC93}$, such as $bamA^{ECL}$ or one of the mutants isolated in this study.

In summary, the CDI pathway of *Escherichia coli* EC93 depends on CdiA binding to a few specific residues in loops 4, 6, and 7 on the extracellular face of BamA. These residues do not appear to be important for individual cell viability, and yet BamA extracellular loops are highly conserved in *E. coli* subspecies. This supports the hypothesis that CDI plays a broader ecological role, such as kin selection during the formation of bacterial communities.

MAMKKLLIASLLFSSATVYGAEGFVVKDIHFEGLQRVAVGAALLSMPVRTGDTVNDEDISNTIRAL

FATGNFEDVRVLRDGDTLLVQVKERPTIASITFSGNKSVKDDMLKQNLEASGVRVGESLDRTTIA

DIEKGLEDFYYSVGKYSASVKAVVTPLPRNRVDLKLVFQEGVSAEIQQINIVGNHAFTTDELISHF

QLRDEVPWWNVVGDRKYQKQKLAGDLETLRSYYLDRGYARFNIDSTQVSLTPDKKGIYVTVNIT

EGDQYKLSGVEVSGNLAGHSAEIEQLTKIEPGELYNGTKVTKMEDDIKKLLGRYGYAYPRVQSM

PEINDADKTVKLRVNVDAGNRFYVRKIRFEGNDTSKDAVLRREMRQMEGAWLGSDLVDQGKER

L1

LNRLGFFETVDTDTQRVPGSPDQVDVVYKVKERNTGSFNFGIGYGTESGVSFQAGVQQDNWL

L2 **L3**

GTGYAVGINGTKNDYQTYAELSVTNPYFTVDGVSLGGRLFYNDFQADDADLSDYTNKSYGTDVT

L4

LGFPINEYNSLRAGLGYVHNSLSNMQPQVAMWRYLYSMGEHPSTSDQDNSFKTDDFTFNYGW

L5

TYNKLDRGYFPTDGSRVNLTGKVTIPGSDNEYYKVTLDTATYVPIDDDHKWVVLGRTRWGYGD

L6

GLGGKEMPFYENFYAGGSSTVRGFQSNTIGPKAVYFPHQASNYDPDYDYECATQDGAKDLCKS

L7

DDAVGGNAMAVASLEFITPTPFISDKYANSVRTSFFWDMGTVWDTNWDSSQYSGYPDYSDPSN

L8

IRMSAGIALQWMSPLGPL VFSYAQPFKKYDGDKAEQFQFNIGKTW

Figure 2.1. Sequence of BamA from Escherichia coli. Loop 4 (L4), cyan; Loop 6 (L6), red; Loop 7 (L7), purple; other extracellular loops, grey. Mutated residues are bolded in dark blue; 10-residue deletion ΔA672_N681 is underlined. The α-helix of L4 is annotated.

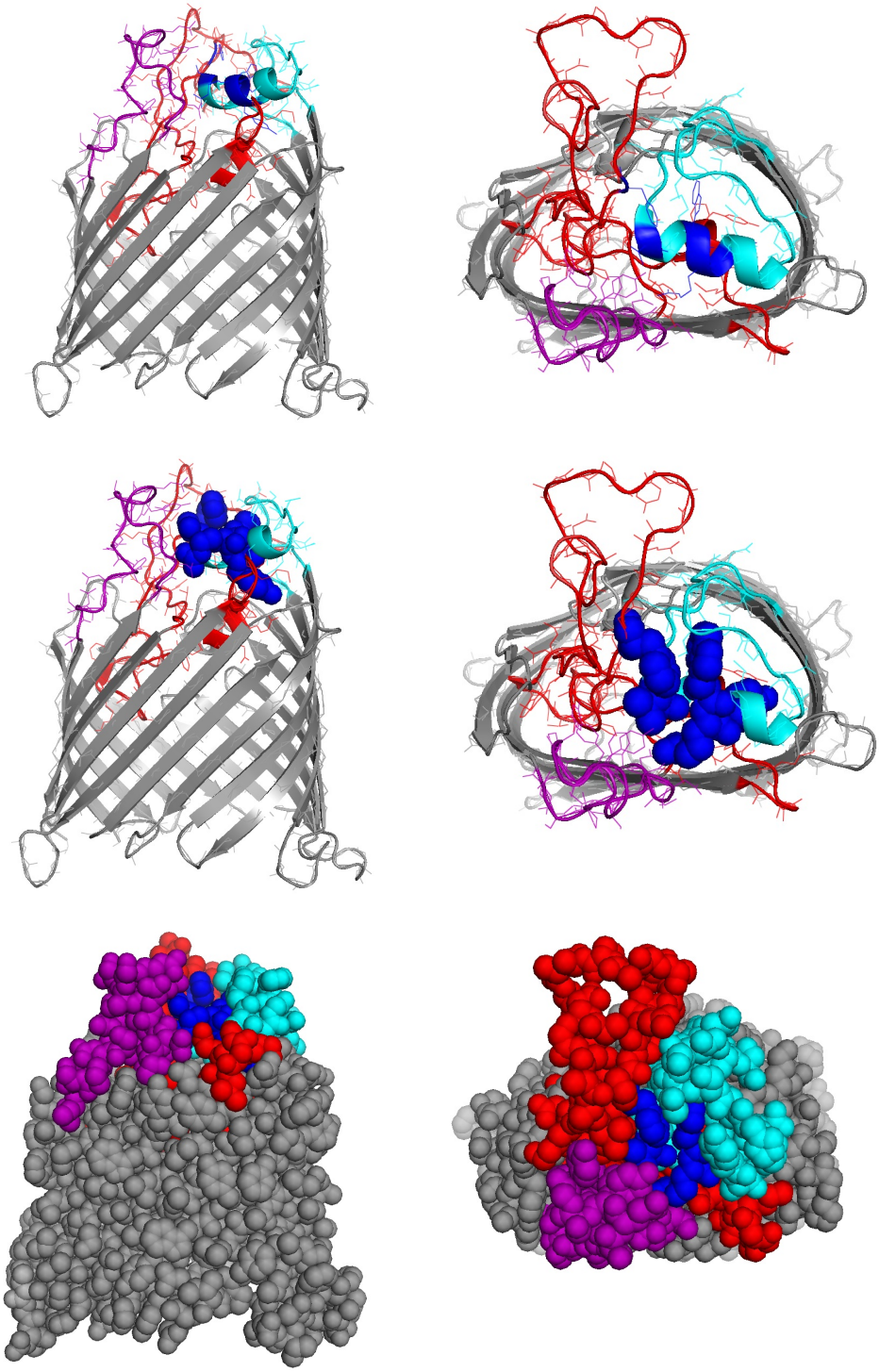

Figure 2.2. Location of mutations in BamA. Images were generated in PyMol using a previously published structure of BamA (PDB: 4N75). Left column: side view, with lateral pore in background and extracellular loops on top. Right column: top view, with extracellular loops in foreground. Loop 4, cyan; Loop 6, red; Loop 7, purple; mutated residues, dark blue.

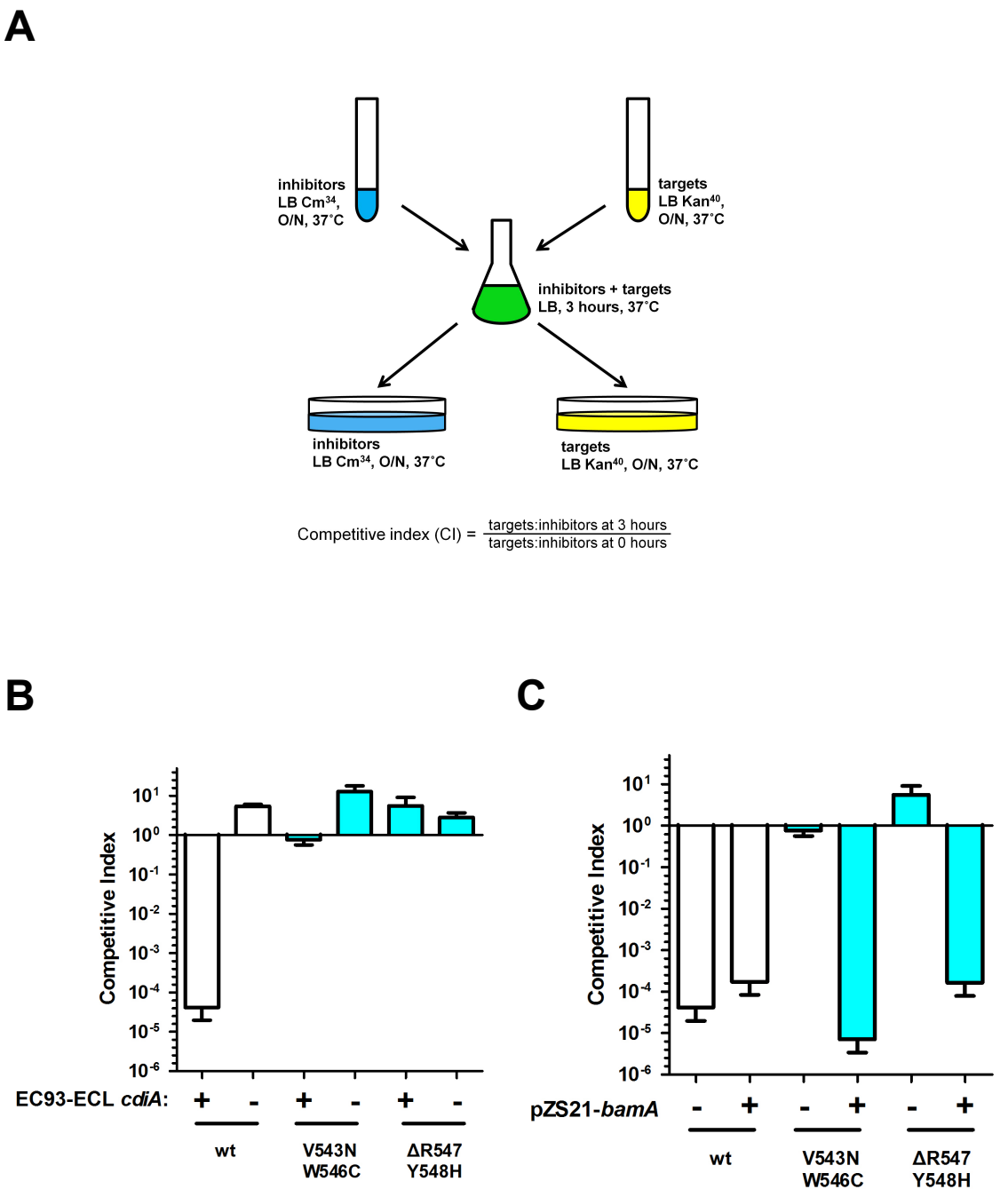

Figure 2.3. *bamA* loop 4 mutations confer resistance to EC93-ECL chimeric CDI system. (A) Diagram of growth-competition assay. O/N, overnight. (B) Competitions between *E. coli* carrying either plasmid-borne EC93-ECL chimeric CDI system (+) or empty vector (-), and *E. coli bamA* loop 4 mutants. (C) Complementation with pZS21-*bamA* (+) restores sensitivity of *bamA* loop 4 mutants to CDI. Competitions between *E. coli* carrying EC93-ECL chimeric CDI system and *E. coli bamA* loop 6 mutants +/- complementation vector pZS21-*bamA*-amp (Table 2.3). Data represent the mean ± SEM for two independent experiments.

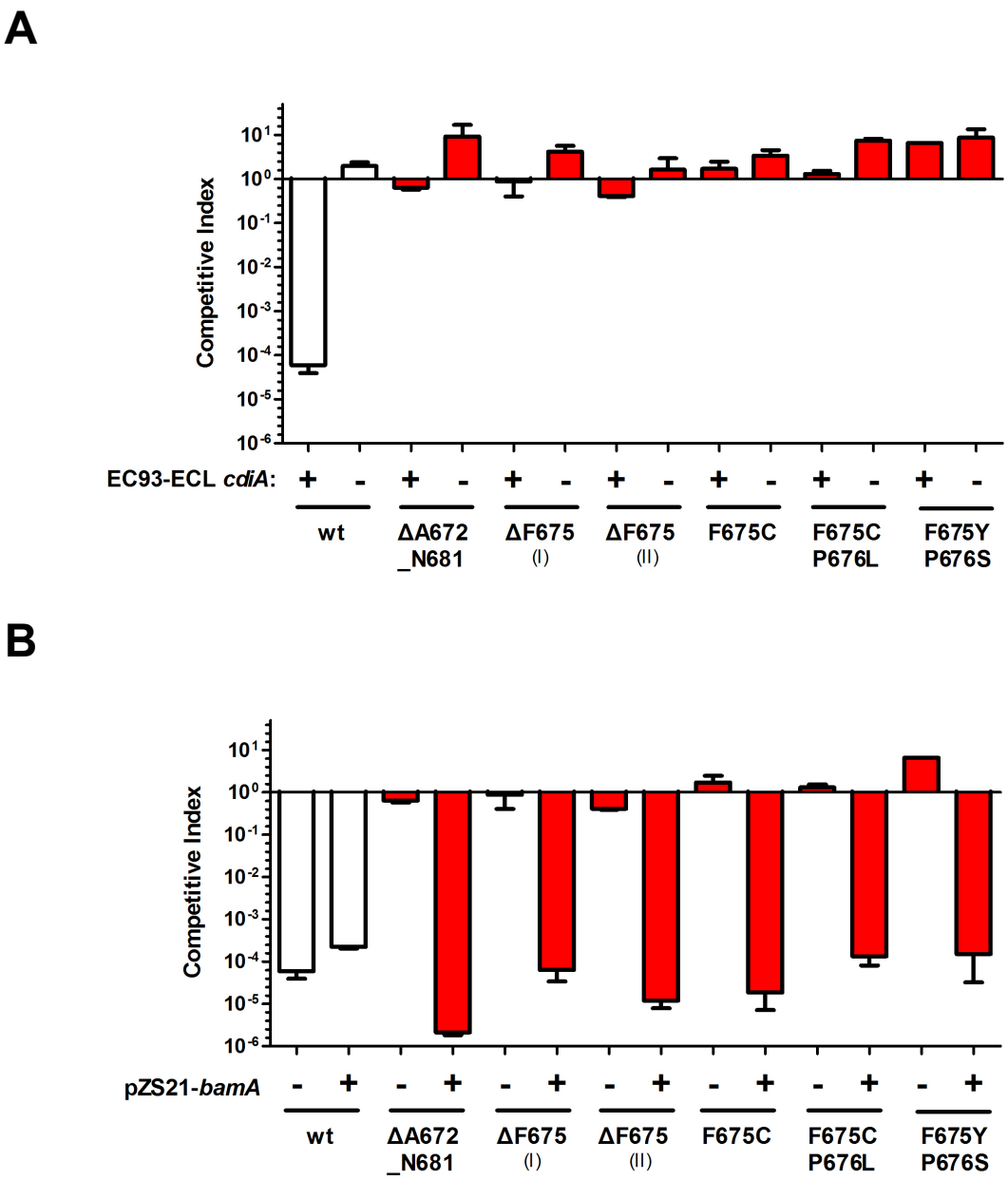

Figure 2.4. *bamA* loop 6 mutations confer resistance to EC93-ECL chimeric CDI system. (A) Competitions between *E. coli* carrying either plasmid-borne EC93-ECL chimeric CDI system (+) or empty vector (-), and *E. coli bamA* loop 6 mutants. (B) Complementation with pZS21-*bamA* (+) restores sensitivity of *bamA* loop 6 mutants to CDI. Competitions between *E. coli* carrying EC93-ECL chimeric CDI system and *E. coli bamA* loop 6 mutants +/- complementation vector pZS21-*bamA*-amp (Table 2.3). Data represent the mean ± SEM for two independent experiments.

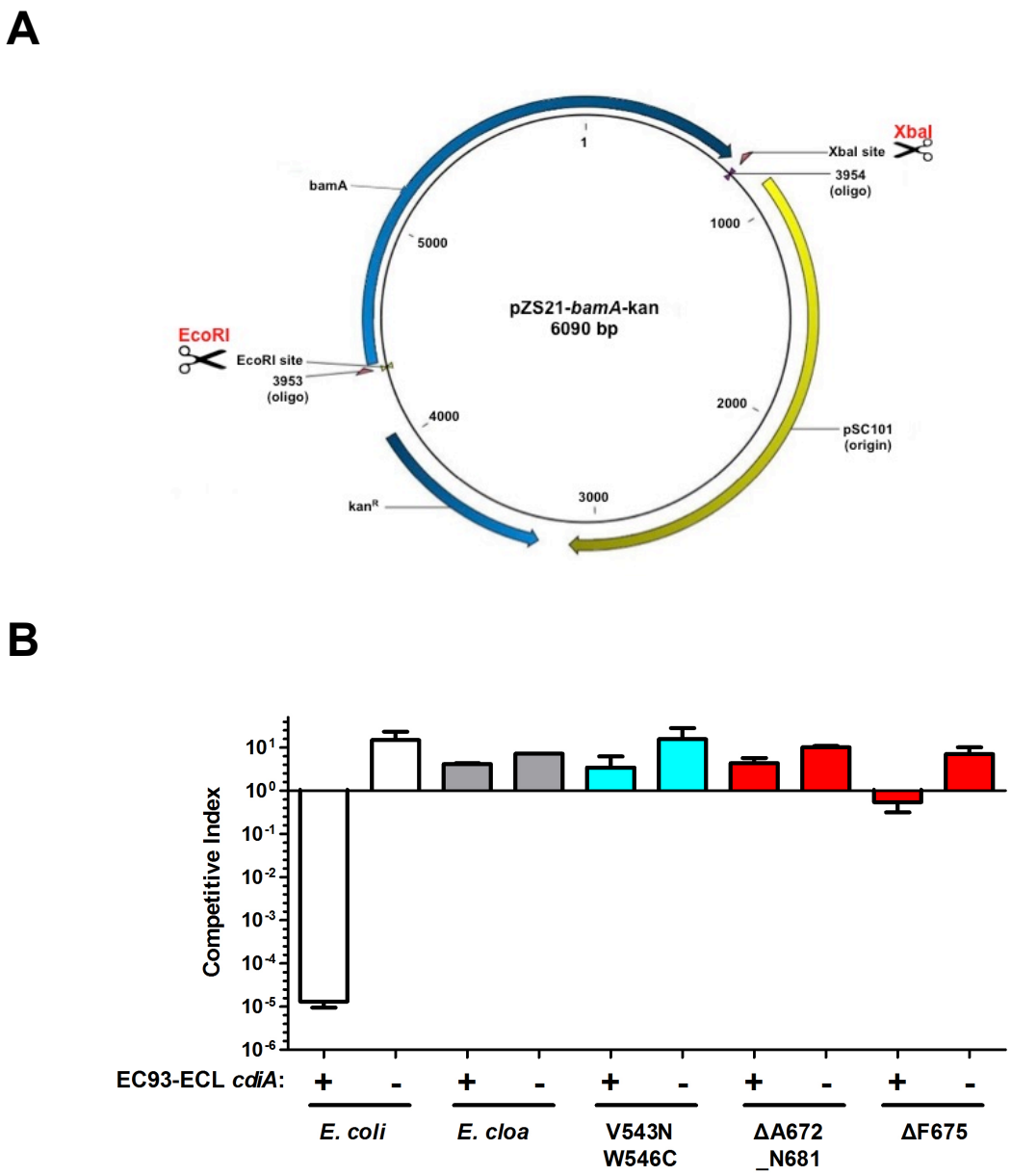

Figure 2.5. Introducing *bamA* mutations into pZS21. (A) Diagram of pZS21-*bamA*-kan. kan^{R}, kanamycin resistance gene; in pZS21-*bamA*-amp, this is replaced by an ampicillin resistance gene. The plasmid was cut at the EcoRI and XbaI sites to excise the wild-type *bamA* allele and ligate in mutant *bamA* alleles. (B) Competitions between *E. coli* carrying either plasmid-borne CDI^{EC93} (+) or empty vector (-), and *E. coli bamA::cat* targets expressing mutant *bamA* alleles from pZS21. Loop 4 mutant, cyan; loop 6 mutants, red. Data represent the mean ± SEM for two independent experiments.

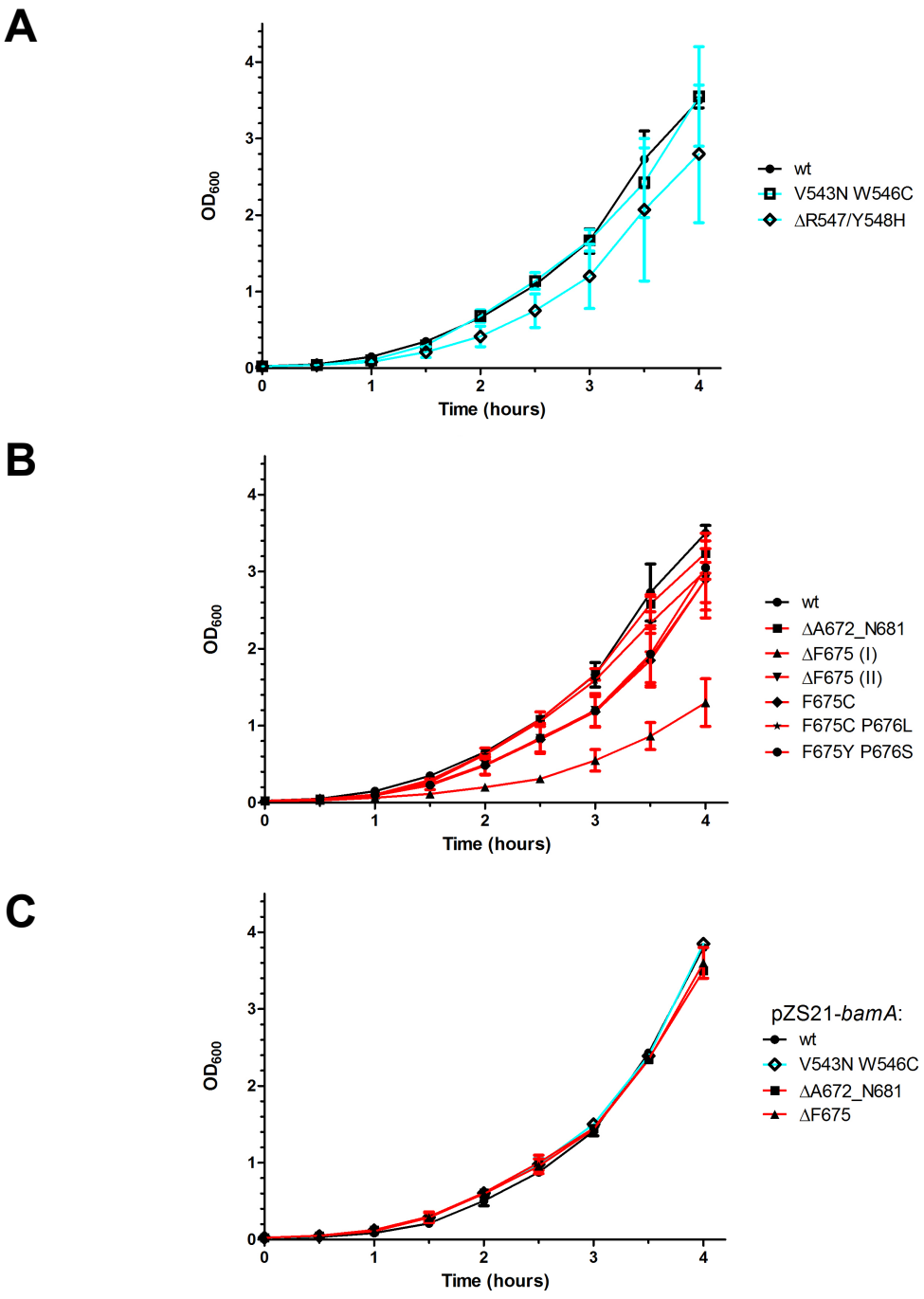

Figure 2.6. Growth curves of *bamA* mutants. OD_{600} was measured every 30 minutes. (A) Loop 4 mutants, cyan. (B) Loop 6 mutants, red. (C) *bamA* alleles expressed from pZS21 in an *E. coli bamA::cat* background (Table 2.2).

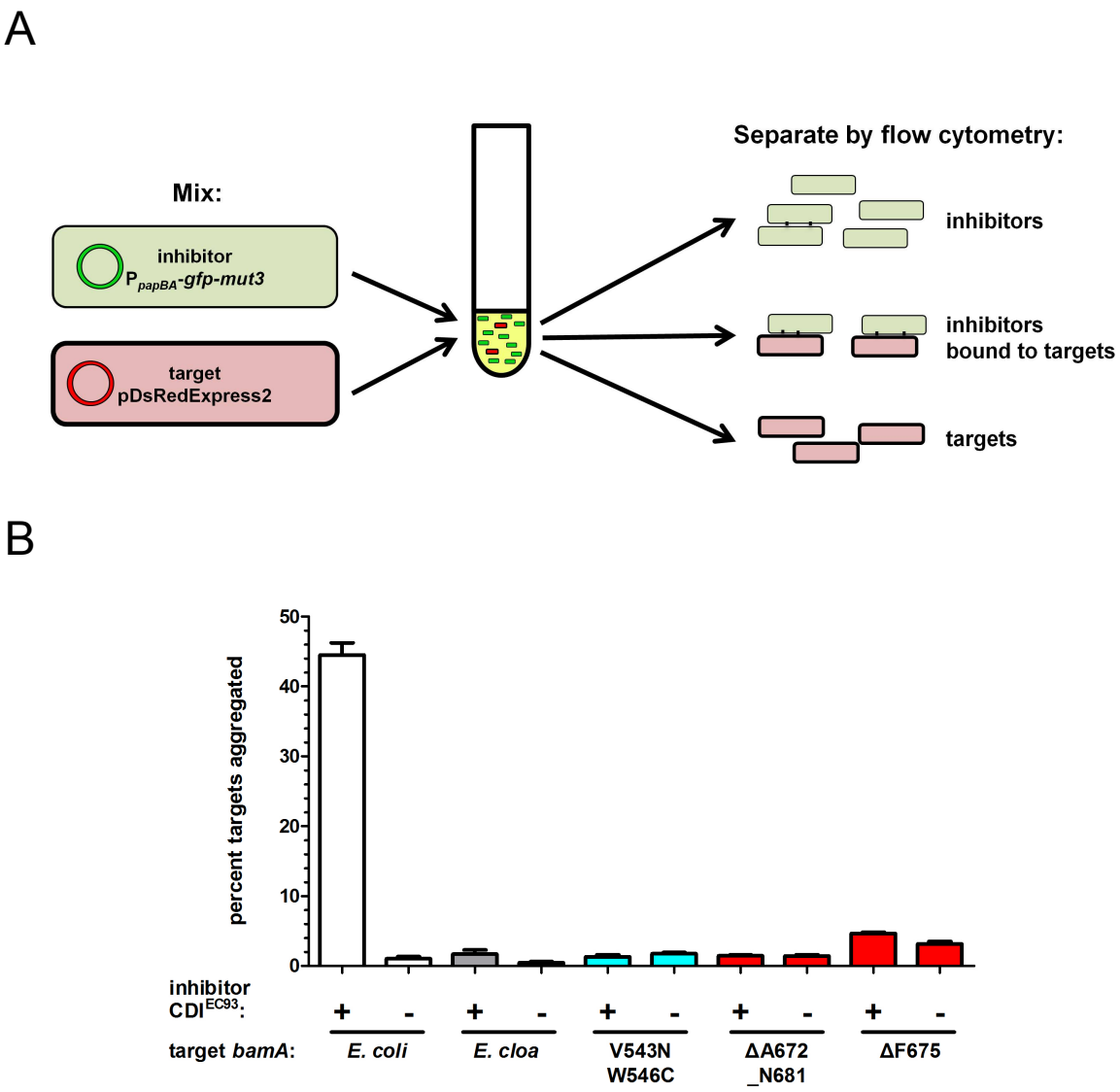

Figure 2.7. Mutations in *bamA* block cell-cell binding. (A) Diagram of binding assays. DL4905 and DL4906 inhibitor cells express *gfp* constitutively from the chromosome (Table 2.2). Target cells were transformed with pDsRedExpress2, and overnight cultures were inoculated from red colonies. Inhibitors were co-cultured in 4-fold excess with targets and analyzed by flow cytometry. (B) Adhesion between inhibitors and targets. Percent targets aggregated denotes the percentage of red-fluorescent cells aggregated with green-fluorescent inhibitors. Loop 4 mutant, cyan; loop 6 mutants, red. Data represent the mean ± SEM for three independent experiments.

Mutation	Source	Location
V543N/W546C	UV	loop 4 helix
ΔR547/Y548H or R547H/ΔY548	UV	loop 4 helix
ΔA672_N681	spontaneous	loop 6
ΔF675	UV	loop 6
F675C	spontaneous	loop 6
F675C/P676L	UV	loop 6
F675Y/P676S	UV	loop 6

Table 2.1. Mutations in *bamA*. ΔF675 appeared in two independent mutagenesis experiments. All mutations isolated from mutant pools exposed to UV, except for ΔA672_N681 and F675C, which are presumed to be spontaneous. ΔA672_N681 was isolated during a transposon mutagenesis experiment and has an insertion upstream of *yjfY* that is not linked to CDI resistance. F675C was isolated from a control pool not exposed to UV.

Table 2.2. Bacterial strains used in this study.

Strains	Description[a]	Source or Reference
EPI100	F- *mcrA Δ(mrr-hsdRMS-mcrBC) Φ80dlacZΔM15 ΔlacX74 recA1 endA1 araD139 Δ(ara, leu)7697 galU galK λ⁻ rpsL (Str^R) nupG*	Epicentre
MC4100	F$^-$ *araD139* Δ*lacU169 rpsL150 relA1 flb5301 deoC1 ptsF25 rbsR*	[74]
CH9702	EPI100 Δ*bamA::cat* pZS21-*bamA*^{Ecoli} pDsRedExpress2, Kan^R Amp^R	[18]
CH9703	EPI100 Δ*bamA::cat* pZS21-*bamA*^{ECL} pDsRedExpress2, Kan^R Amp^R	[18]
DL4527	EPI100 pWEB-TNC, Cm^R	[2]
DL4905	MC4100 λ640-13 P$_{papBA}$-*gfp-mut3* pDAL660Δ1-39	[12,18]
DL4906	MC4100 λ640-13 P$_{papBA}$-*gfp-mut3*, pWEB::TNC, Amp^R Kan^R	[18]
DL5562	JCM158 *wzb::kan*, Kan^R	[12]
DL5564	JCM158 Δ*wzb*	[12]
DL6815	MC4100 *bamA::cat* pZS21-*bamA*^{ECL}-kan, Kan^R	[18]
DL6916	MC4100 *bamA::cat* pZS21-*bamA*^{Ecoli}-kan, Kan^R	[18]
DL6917	MC4100 *bamA::cat* pZS21-*bamA*^{Ecoli}-amp, Amp^R	[18]
DL8680	EPI100 pCH10445, Cm^R	[7]
DL8686	EPI100 pTrc99a::*cdiI*^{ECL}, Amp^R	[7]
DL8690	DL5562 *bamA*$^{\Delta A672\_681}$, Kan^R	This study
DL8738	DL5562 *bamA*$^{\Delta F675}$ (i), Kan^R	This study
DL8751	DL5562 *bamA*$^{F675C/P676L}$, Kan^R	This study
DL8753	DL5562 *bamA*$^{V543N/W546C}$, Kan^R	This study
DL8763	DL5562 *bamA*$^{\Delta R547/Y548H}$, Kan^R	This study
DL8804	MC4100 *bamA::cat* pZS21-*bamA*$^{\Delta A672\_681}$-kan, Kan^R	This study
DL8805	MC4100 *bamA::cat* pZS21-*bamA*$^{\Delta F675}$-kan, Kan^R	This study
DL8807	MC4100 *bamA::cat* pZS21-*bamA*$^{V543N/W546C}$-kan, Kan^R	This study
DL8830	DL5562 *bamA*$^{\Delta F675}$ (ii), Kan^R	This study
DL8831	DL5562 *bamA*$^{F676Y/P676S}$, Kan^R	This study
DL8832	DL5562 *bamA*^{F675C}, Kan^R	This study

Table 2.3. Plasmids used in this study.

Plasmid	Description[a]	Source or Reference
pCH10445	Constitutive expression of chimeric *cdiA*^{EC93}-*CT*^{ECL} and *cdiI*^{ECL} genes, Cm^R	[7]
pDsRedExpress2	Constitutive expression of DsRed, Amp^R	[18]
pTrc99a::*cdiI*^{ECL}	IPTG-inducible expression of *cdiI*^{ECL}, AmpR	[7]
pZS21-*bamA*-amp	pZS21 expressing BamA, Amp^R	[12]
pZS21-*bamA*^{Ecoli}-kan	pZS21 expressing BamA from *Escherichia coli*, Kan^R	[59]
pZS21-*bamA*^{ECL}-kan	pZS21 expressing BamA from *Enterobacter cloacae*, Kan^R	[18]

Table 2.4. Oligonucleotides used in this study.

Oligonucleotide	Sequence[b]	Source or Reference
1157	5’ CAT CTG CTG TTC CTT GCG 3’	This study
1168	5' ATC GCA TTG GCT CGA TTC TGC TG 3’	This study
2462	5’ GCA CCT CTG ATC AGG ATA AC 3’	This study
2586	5’ AGG TTG CGA TGT GGC GTT AT 3’	This study
2587	5’ AGA TCG GTT TCC ATA CGC TG 3’	This study
3691	5’ GTT TCA ACA TCG ACT CTA CC 3’	This study
3937	5’ GGT GAA CAT CAC CGA AGG CGA T 3’	This study
3938	5’ CGT TAT CCG ATC CAG GAA TGG 3’	This study
3939	5’ GGT CAC TTT GGT GCC GTT AT 3’	This study
3953	5’ AAA gaattc TAG TTA GGA AGA ACG 3’	This study
3954	5’AAA tctaga CTA AAG TCA TCG CTA CA 3’	This study

[a]Abbreviations: Amp^R, ampicillin-resistant; Kan^R, kanamycin-resistant; Cm^R, chloramphenicol-resistant.

[b]Restriction endonuclease sites are in lowercase.

References

1. Aoki SK, Diner EJ, de Roodenbeke CT, Burgess BR, Poole SJ, Braaten BA, et al. A widespread family of polymorphic contact-dependent toxin delivery systems in bacteria. Nature 2010; 468: 439-442.
2. Aoki SK, Pamma R, Hernday AD, Bickham JE, Braaten BA, Low DA. Contact-dependent inhibition of growth in Escherichia coli. Science 2005; 309: 1245-1248.
3. Ruhe ZC, Low DA, Hayes CS. Bacterial contact-dependent growth inhibition. Trends Microbiol 2013; 21: 230-237.
4. Hayes CS, Koskiniemi S, Ruhe ZC, Poole SJ, Low DA. Mechanisms and biological roles of contact-dependent growth inhibition systems. Cold Spring Harb Perspect Med 2014; 4 pii: a010025.
5. Kajava AV, Cheng N, Cleaver R, Kessel M, Simon MN, Willery E. Beta-helix model for the filamentous haemagglutinin adhesin of Bordetella pertussis and related bacterial secretory proteins. Mol Microbiol 2001; 42: 279-292.
6. Zhang D, Iyer LM, Aravind L. A novel immunity system for bacterial nucleic acid degrading toxins and its recruitment in various eukaryotic and DNA viral systems. Nucleic Acids Res 2011; 39: 4532-4552.
7. Beck CM, Morse RP, Cunningham DA, Iniguez A, Low DA, Goulding CW. CdiA from Enterobacter cloacae delivers a toxic ribosomal RNase into target bacteria. Structure 2014; 22: 707-718.
8. Morse RP, Nikolakakis KC, Willett JL, Gerrick E, Low DA, Hayes CS, et al. Structural basis of toxicity and immunity in contact-dependent growth inhibition (CDI) systems. Proc Natl Acad Sci U S A 2012; 109: 21480-21485.
9. Nikolakakis K, Amber S, Wilbur JS, Diner EJ, Aoki SK, Poole SJ, et al. The toxin/immunity network of Burkholderia pseudomallei contact-dependent growth inhibition (CDI) systems. Mol Microbiol 2012; 84: 516-529.
10. Aoki SK, Webb JS, Braaten BA, Low DA. Contact-dependent growth inhibition causes reversible metabolic downregulation in Escherichia coli. J Bacteriol 2009; 191: 1777-1786.
11. Zhang D, de Souza RF, Anantharaman V, Iyer LM, Aravind L. Polymorphic toxin systems: Comprehensive characterization of trafficking modes, processing, mechanisms of action, immunity and ecology using comparative genomics. Biol Direct 2012; 7: 18.
12. Aoki SK, Malinverni JC, Jacoby K, Thomas B, Pamma R, Trinh BN, et al. Contact-dependent growth inhibition requires the essential outer membrane protein BamA (YaeT) as the receptor and the inner membrane transport protein AcrB. Mol Microbiol 2008; 70: 323-340.
13. Diner EJ, Beck CM, Webb JS, Low DA, Hayes CS. Identification of a target cell permissive factor required for contact-dependent growth inhibition (CDI). Genes Dev 2012; 26: 515-525.
14. Voulhoux R, Bos MP, Geurtsen J, Mols M, Tommassen J. Role of a highly conserved bacterial protein in outer membrane protein assembly. Science 2003; 299: 262-265.

15. Gentle I, Gabriel K, Beech P, Waller R, Lithgow T. The Omp85 family of proteins is essential for outer membrane biogenesis in mitochondria and bacteria. J Cell Biol 2004;164: 19-24.
16. Wu T, Malinverni J, Ruiz N, Kim S, Silhavy TJ, Kahne D. Identification of a multicomponent complex required for outer membrane biogenesis in Escherichia coli. Cell 2005; 121: 235-245.
17. Werner J, Misra R. YaeT (Omp85) affects the assembly of lipid-dependent and lipid-independent outer membrane proteins of Escherichia coli. Mol Microbiol 2005; 57: 1450-1459.
18. Ruhe ZC, Wallace AB, Low DA, Hayes CS. Receptor polymorphism restricts contact-dependent growth inhibition to members of the same species. MBio 2013; 4: 00480-13 [pii].
19. Ma D, Cook DN, Alberti M, Pon NG, Nikaido H, Hearst JE. Genes acrA and acrB encode a stress-induced efflux system of Escherichia coli. Mol Microbiol 1995; 16: 45-55.
20. Anderson MS, Garcia EC, Cotter PA. The Burkholderia bcpAIOB genes define unique classes of two-partner secretion and contact dependent growth inhibition systems. PLoS Genet 2012; 8: e1002877.
21. Poole SJ, Diner EJ, Aoki SK, Braaten BA, t'Kint de Roodenbeke C, Low DA et al. Identification of functional toxin/immunity genes linked to contact-dependent growth inhibition (CDI) and rearrangement hotspot (Rhs) systems. PLoS Genet 2011; 7: e1002217.
22. Arenas J, Schipper K, van Ulsen P, van der Ende A, Tommassen J. Domain exchange at the 3' end of the gene encoding the fratricide meningococcal two-partner secretion protein A. BMC Genomics 2013; 14: 622.
23. Miller VL, Mekalanos JJ. A novel suicide vector and its use in construction of insertion mutations: osmoregulation of outer membrane proteins and virulence determinants in Vibrio cholerae requires toxR. J Bacteriol 1988; 170: 2575-2583.
24. Choi KH, Mima T, Casart Y, Rholl D, Kumar A, Beacham IR, et al. Genetic tools for select-agent-compliant manipulation of Burkholderia pseudomallei. Appl Environ Microbiol 2008 74: 1064-1075.
25. Ditta G, Stanfield S, Corbin D, Helinski DR. Broad host range DNA cloning system for gram-negative bacteria: construction of a gene bank of Rhizobium meliloti. Proc Natl Acad Sci U S A 1980; 77: 7347-7351.
26. Gallagher LA, Ramage E, Patrapuvich R, Weiss E, Brittnacher M, Manoil C. Sequence-defined transposon mutant library of Burkholderia thailandensis. MBio 2013; 4: e00604-00613.
27. Cardona ST, Valvano MA. An expression vector containing a rhamnose-inducible promoter provides tightly regulated gene expression in Burkholderia cenocepacia. Plasmid 2005; 54: 219-228.
28. Hayes CS, Sauer RT. Cleavage of the A site mRNA codon during ribosome pausing provides a mechanism for translational quality control. Mol Cell 2003; 12: 903-911.
29. Barrett AR, Kang Y, Inamasu KS, Son MS, Vukovich JM, Hoang TT et al. Genetic tools for allelic replacement in Burkholderia species. Applied and Environmental Microbiology 2008; 74: 4498-4508.

30. Aiyar A, Xiang Y, Leis J. Site-directed mutagenesis using overlap extension PCR. Methods Mol Biol. 1996; 57: 177-191.
31. Beck CM, Diner EJ, Kim JJ, Low DA, Hayes CS. The F pilus mediates a novel pathway of CDI toxin import. Mol Microbiol 2014; 93: 276-290.
32. Stone JK, Mayo M, Grasso SA, Ginther JL, Warrington SD, Allender CJ, et al. Detection of Burkholderia pseudomallei O-antigen serotypes in near-neighbor species. BMC Microbiol 2012; 12: 250.
33. Tuanyok A, Stone JK, Mayo M, Kaestli M, Gruendike J, Georgia S, et al. The genetic and molecular basis of O-antigenic diversity in Burkholderia pseudomallei lipopolysaccharide. PLoS Negl Trop Dis 2012; 6: e1453.
34. Broadbent SE, Davies MR, van der Woude MW. Phase variation controls expression of Salmonella lipopolysaccharide modification genes by a DNA methylation-dependent mechanism. Mol Microbiol 2010; 77: 337-353.
35. Cota I, Blanc-Potard AB, Casadesus J. STM2209-STM2208 (opvAB): a phase variation locus of Salmonella enterica involved in control of O-antigen chain length. PLoS One 2012; 7: e36863.
36. Seed KD, Faruque SM, Mekalanos JJ, Calderwood SB, Qadri F, Camilli A. Phase variable O antigen biosynthetic genes control expression of the major protective antigen and bacteriophage receptor in Vibrio cholerae O1. PLoS Pathog 2012; 8: e1002917.
37. Noinaj N, Kuszak AJ, Gumbart JC, Lukacik P, Chang H, Easley NC, et al. Structural insight into the biogenesis of beta-barrel membrane proteins. Nature 2013; 501: 385-390.
38. Ruhe ZC, Nguyen JY, Beck CM, Low DA, Hayes CS. The proton-motive force is required for translocation of CDI toxins across the inner membrane of target bacteria. Mol Microbiol 2014; 94: 466-481.
39. Law CJ, Maloney PC, Wang DN. Ins and outs of major facilitator superfamily antiporters. Annu Rev Microbiol 2008; 62: 289-305.
40. Fluman N, Bibi E. Bacterial multidrug transport through the lens of the major facilitator superfamily. Biochim Biophys Acta 2009; 1794: 738-747.
41. Mosbahi K, Lemaitre C, Keeble AH, Mobasheri H, Morel B, James R, et al. The cytotoxic domain of colicin E9 is a channel-forming endonuclease. Nat Struct Biol 2002; 9: 476-484.
42. Mosbahi K, Walker D, James R, Moore GR, Kleanthous C. Global structural rearrangement of the cell penetrating ribonuclease colicin E3 on interaction with phospholipid membranes. Protein Sci 2006; 15: 620-627.
43. Mosbahi K, Walker D, Lea E, Moore GR, James R, Kleanthous C. Destabilization of the colicin E9 Endonuclease domain by interaction with negatively charged phospholipids: implications for colicin translocation into bacteria. J Biol Chem 2004; 279: 22145-22151.
44. Anderson MS, Garcia EC, Cotter PA. Kind discrimination and competitive exclusion mediated by contact-dependent growth inhibition systems shape biofilm community structure. PLoS Pathog 2014; 10: e1004076.
45. Trakulsomboon S, Vuddhakul V, Tharavichitkul P, Na-Gnam N, Suputtamongkol Y, Thamlikitkul, V. Epidemiology of arabinose assimilation in Burkholderia

pseudomallei isolated from patients and soil in Thailand. Southeast Asian J Trop Med Public Health 1999; 30: 756-759.
46. Schwarz S, West TE, Boyer F, Chiang WC, Carl MA, Hood RD. Burkholderia type VI secretion systems have distinct roles in eukaryotic and bacterial cell interactions. PLoS Pathog 2010; 6: e1001068.
47. Burtnick MN, Brett PJ, Harding SV, Ngugi SA, Ribot WJ, Chantratita, N, et al. The cluster 1 type VI secretion system is a major virulence determinant in Burkholderia pseudomallei. Infect Immun 2011; 79: 1512-1525.
48. Toesca IJ, French CT, Miller JF. The Type VI secretion system spike protein VgrG5 mediates membrane fusion during intercellular spread by pseudomallei group Burkholderia species. Infect Immun 2014; 82: 1436-1444.
49. Schwarz S, Singh P, Robertson JD, LeRoux M, Skerrett SJ, Goodlett, DR, et al. VgrG-5 is a Burkholderia type VI secretion system-exported protein required for multinucleated giant cell formation and virulence. Infect Immun 2014; 82: 1445-1452.
50. Hood RD, Singh P, Hsu F, Guvener T, Carl MA, Trinidad, RR, et al. A type VI secretion system of Pseudomonas aeruginosa targets a toxin to bacteria. Cell Host Microbe 2010; 7: 25-37.
51. Zheng J, Ho B, Mekalanos JJ. Genetic analysis of anti-amoebae and anti-bacterial activities of the type VI secretion system in Vibrio cholerae. PLoS One 2011; 6: e23876.
52. MacIntyre DL, Miyata ST, Kitaoka M, Pukatzki S. The Vibrio cholerae type VI secretion system displays antimicrobial properties. Proc Natl Acad Sci U S A 2010; 107: 19520-19524.
53. Waterhouse AM, Procter JB, Martin DM, Clamp M, Barton GJ. Jalview Version 2--a multiple sequence alignment editor and analysis workbench. Bioinformatics 2009; 25: 1189-1191.
54. Brett PJ, DeShazer D, Woods DE. Burkholderia thailandensis sp. nov., a Burkholderia pseudomallei-like species. Int J Syst Bacteriol 1998; 48 Pt 1: 317-320.
55. Hoang TT, Karkhoff-Schweizer RR, Kutchma AJ, Schweizer HP A broad-host-range Flp-FRT recombination system for site-specific excision of chromosomally-located DNA sequences: application for isolation of unmarked Pseudomonas aeruginosa mutants. Gene 1998; 212: 77-86.
56. Ruhe ZC, Townsley L, Wallace AB, King A, Van der Woude MW, et al. CdiA promotes receptor independent intercellular adhesion. Mol Microbiol 2015; doi: 10.1111/mmi.13114. [Epub ahead of print]
57. Noinaj N, Rollauer SE, Buchanan SK. The β-barrel membrane protein insertase machinery from Gram-negative bacteria. Curr Opin Struct Biol 2015; 31: 35-42.
58. Kim KH, Aulakh S, Paetzel M. The bacterial outer membrane β-barrel assembly machinery. Protein Sci 2012; 21: 751-756.
59. Kim S, Malinverni JC, Sliz P, Silhavy TJ, Harrison SC, Kahne D. Structure and function of an essential component of the outer membrane protein assembly machine. Science 2007; 317: 961-964.
60. Ni D, Wang Y, Yang X, Zhou H, Hou X, et al. Structural and functional analysis of the β-barrel domain of BamA from Escherichia coli. FASEB J 2014; 28: 2677-2685.

61. Albrecht R, Schütz M, Oberhettinger P, Faulstich M, Bermejo I, et al. Structure of BamA, an essential factor in outer membrane protein biogenesis. Acta Crystallogr D Biol Crystallogr 2014; 70: 1779-1789.
62. Clantin B, Delattre AS, Rucktooa P, Saint N, Méli AC, et al. Structure of the membrane protein FhaC: a member of the Omp85-TpsB transporter superfamily. Science 2007; 317: 957-961.
63. Smith DL, James CE, Sergeant MJ, Yaxian Y, Saunders JR, et al. Short-tailed stx phages exploit the conserved YaeT protein to disseminate Shiga toxin genes among enterobacteria. J Bacteriol 2007; 189: 7223–7233.
64. Imamovic L, Martínez-Castillo A, Benavides C, Muniesa M. BaeSR, involved in envelope stress response, protects against lysogenic conversion by Shiga toxin 2-encoding phages. Infect Immun 2015; 83: 1451-1457.
65. Delattre AS, Clantin B, Saint N, Locht C, Villeret V, et al. Functional importance of a conserved sequence motif in FhaC, a prototypic member of the TpsB/Omp85 superfamily. FEBS J 2010; 277: 4755-4765.
66. Noinaj N, Kuszak AJ, Balusek C, Gumbart JC, Buchanan SK. Lateral opening and exit pore formation are required for BamA function. Structure 2014; 22: 1055-1062.
67. Leonard-Rivera M, Misra R. Conserved residues of the putative L6 loop of Escherichia coli BamA play a critical role in the assembly of β-barrel outer membrane proteins, including that of BamA itself. J Bacteriol 2012; 194: 4662-4668.
68. Webb JS, Nikolakakis KC, Willett JL, Aoki SK, Hayes CS, et al.. Delivery of CdiA nuclease toxins into target cells during contact-dependent growth inhibition. PLoS ONE 2013; 8: e57609.
69. Willett JL, Gucinski GC, Fatherree JP, Low DA, Hayes CS. Contact-dependent growth inhibition toxins exploit multiple independent cell-entry pathways. Proc Natl Acad Sci U S A 2015; doi: 10.1073/pnas.1512124112. [Epub ahead of print]
70. Chung CT, Niemela SL, Miller RH. One-step preparation of competent Escherichia coli: Transformation and storage of bacterial cells in the same solution. Proc Nat Acad Sci U S A 1989; 86: 2172-2175.
71. Chiang SL, Rubin EJ. Construction of a mariner-based transposon for epitope-tagging and genomic targeting. Gene 2002; 296: 179-185.
72. Cascales E, Buchanan SK, Duché D, Kleanthous C, Lloubès R, et al. Colicin biology. Microbiol Mol Biol Rev 2007; 71: 158-229.
73. Sinnige T, Weingarth M, Renault M, Baker L, Tommassen J, et al. Solid-state NMR studies of full-length BamA in lipid bilayers suggest limited overall POTRA mobility. J Mol Biol 2014; 426: 2009–2021.
74. Casadaban MJ. Regulation of the regulatory gene for the arabinose pathway, *araC*. J Mol Biol 1976; 104: 557-566.